PKC-alpha regulates the phosphorylation of KRAS that suppresses its oncogenic properties

Tejashree Joglekar,[1,2] Albert Ku,[1,2] Ethan Schollaert,[1,2] Yi-Nan Gong,[1,3]

Jacob Stewart-Ornstein,[4] Anatoly Urisman,[5]

and Man-Tzu Wang*[1,2]

[1]Tumor Microenvironment Center, UPMC Hillman Cancer Center, Pittsburgh, PA 15213, USA

and

[2]Department of Pharmacology and Chemical Biology, University of Pittsburgh, Pittsburgh, PA, 15213, USA

and

[3]Department of Immunology, University of Pittsburgh, Pittsburgh, PA, 15213, USA

and

[4]Department of Computational and Systems Biology, University of Pittsburgh, Pittsburgh, PA, 15213, USA

and

[5]Helen Diller Family Comprehensive Cancer Center

University of California

San Francisco, CA 94158, USA

and

*Correspondence and requests for materials should be addressed to M-T Wang (email: wangm7@upmc.edu or wangmt@pitt.edu).

Summary

KRAS-calmodulin (CaM) signaling axis reportedly regulates the oncogenic properties of KRAS. Phosphorylation of KRAS by PKC uncouples KRAS-CaM and consequently suppresses KRAS-driven malignancies. However, broadly activating PKC could mediate tumor promoting signaling nodes and cause systemic toxicity, diming its applicability as an anti-KRAS therapy. Here, we found that prostratin, but not byrostatin, specifically mediates KRAS phosphorylation, resulting in an elevated level of active CaM in the cytosol and suppresses malignancies of KRAS mutant cells. A whole-genome wide CRISPR/Cas9 knockout screening followed by biochemistry approaches revealed that prostratin acts through activating PKCα. Functional studies confirmed PKCα as the key kinase to phosphorylate KRAS and, therefore, a KRAS suppressor. Activated PKCα induced senescence in KRAS mutant tumor cells through PTPN14, accompanied by a secretory phenotype contributing to the growth inhibition. Our findings reveal a previously understudied regulation of KRAS-CaM axis by PKCα, which can be an actionable target for developing anti-KRAS therapeutics.

Introduction

Mutant RAS acts as a *bona fide* cancer driver in one-third of human cancers, generally accompanied by a dismal prognosis; consequently, mutant RAS is an attractive therapeutic target. The sequence of the first 165 amino acids in the three RAS isoforms, H-, N-, and K-RAS, whose mutations are directly linked to carcinogenesis, is highly homologous and determines their activity for signal transduction through canonical signaling pathways. However, the mutations in each RAS isoform show high tissue specificity suggesting that the different RAS isoforms may dictate distinct oncogenic outputs. KRAS is the most frequently mutated isoform among the three cancer-associated RAS family members and is preferentially linked to the three deadliest cancers, namely lung, colon, and pancreatic adenocarcinomas; thus, oncogenic KRAS is a major target in anticancer drug discovery (McCormick, 2015; Waters and Der, 2018). Because of its small size and compact structure, KRAS contains no accessible pocket where a drug can bind with high affinity, and thus no KRAS-specific inhibitors have been approved for cancer treatment. Till recently, compounds targeting KRAS-G12C have entered clinical trials and showed promising response rates in patients with non-small cell lung cancers (NSCLCs) (Canon et al., 2019; Fell et al., 2020; Hallin et al., 2020; Hobbs et al., 2016; McCormick, 2020). While this breakthrough validates KRAS as a strong target for intervention, some studies suggest that a subpopulation of KRAS mutant lung cancer cells can bypass the tumor-suppressive effects of KRAS-G12C inhibitors, leading to therapeutic resistance and potential recurrence (Xue et al., 2020). Therapeutic approaches inhibiting other mutant forms of KRAS, such as G12D (the most common mutation in pancreatic ductal adenocarcinoma (PDAC) and in never-smoker patients with NSCLC), G12V, and Q61, remain unavailable (Dogan et al., 2012; Stinchcombe and Der, 2011; Zeitouni et al., 2016). Furthermore, a recent clinical trial has revealed that a subset of patients treated with KRAS-G12C inhibitor unfortunately acquired hotspot mutations in KRAS, including G12V and G12D (Zhao et al., 2021). New approaches are therefore urgently needed to suppress the malignancies driven by aberrancies across the mutational spectrum of KRAS.

Inhibition of canonical RAS effector downstream pathways, such as the MEK/ERK and PI3K/AKT pathways, has long been a popular alternative anti-KRAS approach and is undergoing clinical evaluation, but its efficacy and applicability has been limited by nonspecific cytotoxicity, incomplete inhibition of targeted effectors, and rebound activation of parallel signaling pathways (Cox and Der, 2002; Ryan et al., 2015). Identification of the regulatory activators or downstream signaling effectors specific and essential to the oncogenic output of KRAS may, therefore, facilitate the design of inhibitors to suppress KRAS-driven malignancies with minimized unwanted systemic toxicity.

Despite the tissue-restricted spectrum of its mutations, KRAS is expressed broadly across different anatomical regions, with low tissue specificity. This difference suggests that mutations in particular RAS isoforms potentially dictate unique oncogenic features. Indeed, we previously defined that KRAS4B (abbreviated KRAS hereafter) promotes cancer stem cell (CSC)-like properties, an effect that cannot be reproduced by other RAS isoforms (Wang et al., 2015). Importantly, these CSC-like properties cannot be reproduced in tumor models where an *HRAS* allele is knocked into the *KRAS* locus, suggesting that activating mutations in *KRAS* indeed translate into a distinct functional output in cancers and are not simply a reflection of a selective genetic predisposition influenced by gene-specific regulatory elements (Wang et al., 2015). From protein-structural point of view, only the flexible C-terminal hypervariable region (HVR) can distinguish KRAS from its closely related H- and N-RAS isoforms. Yet, little is known about whether the HVR domain dictates the oncogenic functions and signaling activity specifically mediated by KRAS. We further defined that the binding of KRAS to calmodulin (CaM) through its unique C-terminus determines its unique oncogenic properties. Phosphorylation of KRAS at serine 181, which is essential for this interaction, can dissociate the KRAS-CaM interaction and sequentially block the oncogenic functions of KRAS in human cancers (Alvarez-Moya et al., 2010).

Protein kinase C (PKC) has been shown to phosphorylate KRAS at serine 181 (Ballester et al., 1987; Beans et al., 2013; Bivona et al., 2006). In the initial discovery, Bivona et al. have suggested that PKC agonist can suppress the growth of KRAS mutant cells and, in theory, be conveniently used as an

anti-KRAS drug. Echoing their study, our previous study has used prostratin, a non-tumor-promoting PKC activator (Beans et al., 2013), to demonstrate that activating PKC can block the KRAS-CaM interaction and suppress oncogenic KRAS-driven malignancies (Wang et al., 2015). However, PKC family which contains 13 different isozymes has long been considered oncoproteins due to the unambiguous tumor-promoting function of their potent ligands—phorbol esters—and the prevalence of PKC mutations in human cancers (Spitaler and Cantrell, 2004). Indeed, activation of PKC promotes a broad range of signaling pathways involved in tumor promotion and/or acute systemic toxicity (Garg et al., 2014; Kolczynska et al., 2020; Sims et al., 2014), diminishing the enthusiasm for developing PKC agonists as an anti-KRAS therapy.

Shifting the established paradigm, recently, a study revealed unexpected loss-of-function (LOF) mutations in PKC and their tumor-suppressing function in cancer cells (Antal et al., 2015). In addition, LOF mutations in certain PKC isoforms show an association with oncogenic mutations in KRAS in human cancers (Antal et al., 2015). Indeed, in our prior study, while prostratin suppresses the malignancy of KRAS mutant pancreatic cancer cells both *in vitro* and *in vivo*, the pan-PKC activator phorbol 12-myristate 13-acetate (PMA) does not exhibit the same antitumor effects (Wang et al., 2015). This observation suggests that prostratin, unlike PMA, may activate specific PKC isozymes that preferentially phosphorylate KRAS at serine 181. Therefore, activation of a specific PKC isozyme may be a novel approach to rewire the KRAS-mediated signaling pathway and consequently suppress its oncogenic effects in human cancers while minimizing the off-target effects on activation of other tumor promoting signaling pathways and/ or toxicity.

To address the aforementioned knowledge gap, we utilized prostratin, a PKC agonist that exhibited an unexpected anti-KRAS activity, to show that the phosphorylation of KRAS is specifically mediated by the activation of PKCα. Importantly, we uncovered that prostratin, but not other non-tumor-promoting PKC activators, bryostatin in specific, preferentially activates PKCα and selectively suppresses the growth of KRAS mutant tumor cells.

RESULTS

Prostratin Selectively Inhibits Mutant KRAS-Driven Malignancies. In our previous report, we used prostratin as a proof-of-concept compound to demonstrate that the activation of PKC significantly prevents tumor initiation and growth mediated by oncogenic KRAS in both xenograft and genetically engineered mouse models (Wang et al., 2015). While such antitumor activity has been indicated to be specific to tumors initiated by oncogenic KRAS but not HRAS (Wang et al., 2015), several key questions remain: first, do other nontumorigenic PKC activators, particularly compounds in the well-studied bryostatin family, exhibit the same anti-KRAS effects; and second, does prostratin selectively suppress the malignancies of tumor cells harboring mutant KRAS? We first examined whether bryostatin -I and -II (Fig. 1a, middle and right), can reproduce the anti-KRAS mutant cancer effects of prostratin (Fig. 1a, left). Compounds in the bryostatin family are potent modulators of PKC with potential anticancer and neurological activities (von Burstin et al., 2010; Wender et al., 2008; Wu et al., 2020). Bivona et al. also showed that bryostatin slowed the growth of mouse tumors driven by oncogenic KRAS but not those driven by a phosphorylation deficient KRAS mutant (Bivona et al., 2006).

For a fair comparison of their activities and since PKC activators exhibit a biphasic effect on the activation of PKC –, i.e., they activate PKC to a lesser extent at higher concentrations, we first determined the working concentrations of prostratin, bryostatin I, and bryostatin II for intracellular pan-PKC activation (Fig. 1b). Prostratin at 2 μM, bryostatin I at 1 nM, and bryostatin II at 0.5 nM had comparable abilities to induce PKC activity in two human pancreatic cancer cell lines harboring different KRAS mutations (Fig. 1b). At these working concentrations in 2D culture, bryostatin I and bryostatin II did not show antiproliferative effects, whereas the numbers of viable cells and single cell-derived colonies were significantly reduced upon short-term or long-term prostratin treatments (Fig. 1c-d) in pancreatic and lung cancer cell lines that express different mutant forms of KRAS and display varied KRAS dependencies. In addition, the suppressive effect of prostratin on colony formation was specific to KRAS-G12V-transformed cells and had no effect on cells expressing KRAS-G12V-S181A, which cannot be phosphorylated at serine 181 (Fig. 1d, left panel), confirming our previous observation that

the anti-KRAS activity of prostratin acts through the unique C-terminus of the KRAS protein. It has been increasingly recognized that under some circumstances, *in vitro* 2D and 3D culture systems can result in different bioactivities in cells (Kapalczynska et al., 2018; Lynn et al., 2007). We, therefore, evaluated the effects of prostratin and bryostatin family compounds on the 3D growth of KRAS mutant cancer cells. Compared to the solvent control, prostratin but not bryostatin I or II significantly reduced the ability of pancreatic or lung cancer cells expressing mutant KRAS to grow as viable spheres in 3D culture (Fig. 1e, Extended Data Fig. 1a-b). Notably, human cancer cells expressing wild-type KRAS, as well as a mouse pancreatic adenocarcinoma cell line (iKRAS*), which maintains both wild-type KRAS alleles without doxycycline induction (Collins et al., 2012), were insensitive to prostratin (Fig. 1d). iKRAS* cells with doxycyclin induced expression of mutant KRAS acquired sensitivity to prostratin treatment (Fig. 1d). Taken together, these results suggest that prostratin but not bryostatin I or II selectively suppresses the malignancy of cancer cells harboring constitutively activated KRAS independent of the mutational status in the G domain. Although the HVR domain, which may mediate sensitivity to prostratin, is identical in wild-type KRAS and mutant KRAS, the different responses of tumor cells harboring wild-type and mutant KRAS to prostratin treatment could result from the dependency on the oncogenic activity of KRAS. While most tumor cells expressing mutant KRAS rely heavily on its activity to maintain their malignancy, those in which wild-type KRAS is maintained can be dependent on other driver oncogenes for their survival and growth. In addition, prostratin exerted the greatest suppressive effect on the 2D growth of KRAS mutant cancer cells at 2 to 4 μM, the range of maximal function to activate pan-PKCs via detecting the phosphorylation of a synthetic peptide as a universal substrate (Fig. 1b, Extended Data Fig. 1c).

Accumulating evidence suggests that activation of PKC may promote apoptosis (Lucas and Sanchez-Margalet, 1995; Zhu et al., 2010). However, no evidence indicated that prostratin treatment resulted in apoptosis in various prostratin-responsive cancer cells (Extended Data Fig. 1d). Instead, prostratin induced senescence in oncogenic KRAS-transformed human pancreatic epithelial cells, whereas immortalized cells or oncogenic HRAS-transformed cells showed no changes upon prostratin

treatment (Extended Data Fig. 1e). KRAS mutant cancer cells treated with prostratin exhibited a senescent morphology, significantly increased senescence-associated β-galactosidase (SA-β-Gal) activity, and phenocopied cells treated with both MAPK and CDK4/6 inhibitors, which can reintroduce senescence in KRAS mutant tumor cells (Ruscetti et al., 2018) (Extended Data Fig. 1f-g). In addition, the KRAS mutant tumor cells showed and other senescence-associated markers, such as increased p21 expression (Althubiti et al., 2014) and reduced Lamin B1 expression (Freund et al., 2012; Wang et al., 2017), in response to prostratin treatment but not bryostatin II treatment (Extended Data Fig. 1h).

Prostratin Specifically Induces the Phosphorylation of KRAS and Increases Cytoplasmic CaM Level. We previously showed that prostratin can dissociate the KRAS-CaM interaction (Wang et al., 2015). Disruption of the KRAS-CaM interaction consequentially activated the downstream effector CaMKii, as indicated by its autophosphorylation level, and suppressed the cancer stem cell-like properties uniquely mediated by oncogenic KRAS (Wang et al., 2015) (Fig. 2a). Here, our findings further suggested that prostratin but not other PKC activators, including PMA and bryostatin II, reduced the expression of stem cell markers, such as SOX9 (Christin et al., 2020) and CD44 (Lynn et al., 2007; Seymour et al., 2007), in KRAS mutant cancer cells (Extended Data Fig. 2a-b). Furthermore, prostratin but neither PMA nor bryostatin disrupted the binding of KRAS to CaM in transformed fibroblasts (Fig. 2b) and increased the level of phosphorylated CaMKii in KRAS mutant cancer cells (Fig. 2c, Extended Data Fig. 2a). We then investigated whether prostratin blocks the oncogenic properties of KRAS through its phosphorylation at serine 181. Because no anti-phosphorylated KRAS (phospho-KRAS) antibody is available, and a poly-lysine sequence is located upstream of serine 181 in KRAS (Fig. 2a), which disables efficient trypsin digestion prior to mass spectrometric analysis, we used purified GST-Raf1 Ras-binding domain (RBD), glutathione agarose resin to pull down the active form of KRAS in cells and then performed western blotting specific for phosphoserine. Prostratin treatment increased the level of phosphoserine in cells transformed with KRAS-G12V but not in those transformed with HRAS-G12V, which lacks a similar C-terminal domain for phosphorylation (Fig. 2d), or KRAS-G12V-S181A, which cannot be phosphorylated at serine 181 (Fig. 2e). Importantly, bryostatin did not promote

phosphorylation of KRAS in transformed cells (Fig. 2f). Taken together, these data suggest a unique ability of prostratin to induce phosphorylation of KRAS.

CaM is known to be abundantly present in various types of cells, leading to a potential caveat that the amount of CaM released from KRAS-bound form on the plasma membrane to cytosol may not be sufficient to modulate the subsequent CaM dependent signaling pathways. We then utilized a cytosolic calcineurin reporter (Mehta et al., 2014), whose activity depends on the binding to CaM, to monitor the spatiotemporal subcellular patterns of active CaM upon the stimulation of prostratin. In such assay, CaM that was able to activate calcineurin reporter in cytosolic fraction was significantly increased in the cells treated with prostratin when compared to other PKC activators (Fig. 2 g). These data suggest that the dissociation of KRAS-CaM by prostratin-induced KRAS phosphorylation can alter a downstream CaM-dependent signaling node.

Additionally, prostratin did not cause translocation of KRAS from the cell membrane to the cytoplasm or decrease the phosphorylation of ERK, further suggesting that its tumor-suppressive effect is not caused by loss of the cell membrane-associated form of KRAS (Extended Data Fig. 2c-d).

PKCα is a Key Driver of Prostratin Sensitivity. The abovementioned results suggest that prostratin and other non-tumor-promoting PKC modulators may activate different isozymes in the PKC family, and the specific PKC isozyme preferably activated by prostratin acts as a key kinase to phosphorylate KRAS. To test this possibility and for an unbiased identification of critical PKC isoforms or other potential targets involved in mediating the anti-KRAS activity of prostratin, we performed a genome-wide CRISPR/Cas9 knockout (KO) library screening. The human pancreatic cancer cell line PANC-1, which harbors KRAS-G12D and is sensitive to prostratin treatment, was used as the *in vitro* model for stable expression of the Cas9 protein and a lentiviral pooled CRISPR library containing 76,441 unique single-guide RNAs (sgRNAs). Cells expressing the CRISPR/Cas9 library were then treated with prostratin for 21 days. Knockout of a prostratin sensitivity driver gene could drive the resistance, survival, and proliferation of PANC-1 cells in the continuous presence of prostratin. In our genome-wide screen, knockout of PKCα (encoded by *PRKCA*) strongly rescued survival, whereas other PRKCs were not

identified as strong hits (Fig. 3a, labeled red). Notably, while *KRAS* and many other genes involved in canonical RAS pathways were also among the top 20 highest-ranking candidates (Fig. 3a, labeled blue), knockout of these genes, which are essential for the proliferation and survival of pancreatic tumor cells, may not directly contribute to prostratin resistance.

Prostratin Preferentially Binds and Activates PKCα. The PKC family is a family of isozymes classified into three groups: classical or conventional PKCs, including PKCα; novel PKCs, such as PKCδ; and atypical PKCs. All members contain a conserved kinase domain, but only conventional and novel PKCs contain regulatory domains, which include C1 domains that act as ligand sensors and can bind to most PKC activators, including prostratin and bryostatin (Jiang and Dandekar, 2015; Wender et al., 2011). We then investigated whether prostratin and bryostatin differentially bind to PKC isoforms by using a cellular thermal shift assay (CETSA) (Jafari et al., 2014), which allows us to investigate the thermal stability of proteins upon ligand binding in a cellular setting (Fig. 3b, left panel). Prostratin had a better ability to bind PKCα than bryostatin II, whereas bryostatin II preferentially bound to and stabilized PKCδ in KRAS mutant cancer cells (Fig. 3b, right panel).

The hallmark of PKC activation is its translocation to cellular membranes in response to signal transduction through second messengers. We, therefore, examined whether the stabilization of PKCα by prostratin can directly translate into its activation via re-localization to the cellular membrane. The cell fractionation assay results suggested that prostratin specifically induced the translocation of PKCα from the cytoplasm to the cell membrane in two different KRAS mutant pancreatic cancer cells after short-term (15 minutes) and long-term treatment (48 hours) (Fig. 3c, Extended Data Fig. 3). On the other hand, bryostatin promoted membrane translocation of PKCδ in the same cellular contents (Fig. 3c, Extended Data Fig. 3), consistent with the CETSA results in Fig. 3b**.** Again, neither prostratin nor bryostatin altered the membrane localization of KRAS. Immunofluorescence staining also confirmed that membrane translocation of PKCα was induced by prostratin but not by bryostatin II (Fig. 3d-e). Overall, these results suggest that prostratin and other PKC modulators bind and activate different PKC isoforms in KRAS mutant pancreatic cancer cells.

One potential caveat is that PKCα could be the most predominantly expressed PKC isozyme in KRAS mutant tumor cells and that its expression therefore accordingly affects the cellular responses to prostratin. *In silico* genome-wide transcriptome analysis in multiple tumor cell lines suggested that some tumor cells with PKCδ as the most dominant form of PKC remained highly sensitive to prostratin, further eliminating this possible caveat (Extended Data Fig. 4).

KRAS Is a Substrate of PKCα. We next examined whether KRAS acts as a substrate of PKCα. Immunoprecipitation followed by western blot analysis first confirmed that KRAS was one of the PKC substrates that can be phosphorylated by prostratin-activated PKC at serine residues (Fig. 4a). Furthermore, KRAS protein with a pseudophosphorylation mutation (aspartic acid (Asp)) or phosphorylation-resistant mutation (alanine (Ala)) in the CaM-binding domain (serine 181) no longer functioned as a PKC substrate (Fig. 4a). A direct interaction or binding is essential for kinases to activate their downstream substrates. To investigate the potential interactions between KRAS and PKC isozymes, we first utilized Rasless MEFs (mouse embryonic fibroblasts) with re-expression of either KRAS-G12V or NRAS-G12V. Ras RBD pulldown (PD) followed by western blot analysis indicated that, in Rasless MEFs treated with prostratin, an interaction occurred between PKCα and active KRAS but not NRAS (Fig. 4b). Moreover, this interaction could not be reproduced in the cells treated with bryostatin II, and prostratin did not enhance the interaction between KRAS and PKCδ (Fig. 4b-c). Taken together, these results indicate that KRAS is a downstream substrate of PKCα. Co-transfecting HA-tagged- wild type or constitutively active PKCα with oncogenic H- or -K-RAS in 293T cells, followed by immunoprecipitation of HA, further confirmed the specific interaction between PKCα and KRAS (Fig. 4d). These results suggest that the binding interaction of PKC with KRAS occurs in an isozyme-specific manner.

PKCα Is Essential for the Anti-KRAS Activity of Prostratin. To investigate the function of PKCα in mediating the ability of prostratin to suppress oncogenic KRAS, we established KRAS mutant pancreatic cancer cells in which PKCα was knocked out by CRISPR/Cas9, with or without re-expression (Fig. 5a). In this cell model, depletion of PKCα reduced the level of endogenous phospho-CaMKii

compared to that in control cells expressing Cas9 alone, whereas restoring PKCα expression in the knockout clones increased the level of phospho-CaMKii (Fig. 5a). Furthermore, knocking out PKCα hindered KRAS-CaM dissociation caused by prostratin treatment in KRAS mutant cancer cells (Fig. 5b). In contrast, re-expression of PKCα restored KRAS-CaM dissociation in response to prostratin (Fig. 5b). Moreover, KRAS phosphorylation induced by prostratin in KRAS mutant cancer cells was diminished by a knockout of PKCα and was restored upon re-expression of PKCα (Fig. 5c). More importantly, loss of PKCα desensitized KRAS mutant tumor cells to prostratin treatment in terms of survival and colony formation, and sensitivity to prostratin was restored in cells with restored expression of PKCα (Fig. 5d, Extended Data Fig. 5a).

Among all the cancer cell lines harboring mutant KRAS, MIA PaCa-2 and Panc03.27, with endogenous deletion of PKCα, were outliers and did not respond to prostratin treatment (Extended Data Fig. 5b-c). Overexpression of PKCα significantly sensitized MIA PaCa-2 cells to prostratin (Fig. 5e-g). Taken together, these results confirmed that the intact expression of PKCα is functionally important for prostratin-induced KRAS phosphorylation and the consequent suppression of malignancy in KRAS mutant cancer cells.

PKCα suppresses KRAS-mediated malignancies. Introduction of an HA-tagged constitutively active mutant of PKCα (PKCα-CAT) (Soh and Weinstein, 2003) into PANC-1 cells with PKCα knockout by CRISPR/Cas9 increased the phosphorylation of CaMKii and suppressed colony formation even in the absence of prostratin (Extended Data Fig. 6a; Fig. 6a). The growth inhibition caused by the ectopic expression of PKCα-CAT only occurred in the KRAS mutant tumor cells, but not in the tumor cells harboring wild type KRAS (Extended Data Fig. 6 b-c), resembling the selective suppressive effect of prostratin in tumor cells expressing mutant KRAS. Re-expression of wild type PKCα in MIA PaCa2 cells, which exhibit no detectable endogenous PKCα, significantly suppressed their growth as xenograft tumors (Extended Data Fig. 6d), and knocking out PKCα by CRISPR/Cas9 dramatically increased the growth of PANC-1 xenograft tumors (Fig. 6b), indicating the tumor suppressive role of PKCα in KRAS mutant tumor cells. In addition, knocking out PKCα reduced the tumor initiation frequency in PANC-1

cells when transplanted at lower numbers of tumor cells (0.1 x 10^6 per flank) than the routinely used numbers (reported 1 to 10 x 10^6) (Fig. 6b), indicating that the expression of PKCα may mediate cancer-stem cell like properties in KRAS mutant tumor cells. Overexpression of wild type PKCα or constitutively active PKCα significantly increased cytosol-localized active CaM (Fig. 6c). These results suggest that activated PKCα specifically suppresses the malignancies of KRAS mutant tumor cells and confirm that active PKCα recapitulate the tumor suppressive effect of prostratin.

Activated PKCα induces senescence in KRAS mutant tumor cells. Resembling the effects of prostratin treatment, ectopic expression of constitutively active PKCα suppressed the growth of KRAS mutant cancer cells by inducing cellular senescence, as indicated by SA-β-Gal staining (Fig. 6d). Among all the key mediators of cellular senescence, such as p16, TP53, and p21, the expression of p21 at the protein level was increased in a series of KRAS mutant tumor cells, either treated with prostratin or expressing active PKCα (Fig. 6e; Extended Data Fig. 6e). Such changes in p21 expression also occurred at the transcriptional level (Extended Data Fig. 6f). Cell fractionation assay revealed that there was more nucleus-localized p21, as an indication of functional p21, in the tumor cells expressing active PKCα than control cells (Extended Data Fig. 6g). These data suggest that overexpression or activation of PKCα suppresses the growth of KRAS mutant tumor cells through induction of cellular senescence. Furthermore, the treatment with a CaM inhibitor, W7, blocked the increase in p21 expression caused by the pharmacologically activated PKCα in human pancreatic cancer cells (Extended Data Fig. 6h), suggesting that CaM is involved in the cellular senescence triggered by activated PKCα in the KRAS mutant tumor cells.

PTPN14 mediates the PKCα induced senescence. Identifying the key downstream effector to mediate PKCα-induced senescence in KRAS mutant cells may enable us to design alternative anti-KRAS therapeutic strategies to recapitulate the effects of activating PKCα while minimizing the potential tumor promoting effects driven by PKCα. Thus, we used siRNAs to knock down top 5 genes, excluding PKCα, KRAS, and other canonical RAS signaling nodes, from our genome-wide KO library screening (Fig. 3a). We also included p38 MAPK (*MAPK11*) because activation of p38 MAPK signaling has been

reported to be involved in PKCα-mediated tumor suppression and cellular senescence in oncogenic KRAS-induced lung cancer (Hill et al., 2014). With comparable knockdown efficiency (Extended Data Table 1), only depletion of PTPN14 compromised the senescence program including increased senescence associated β-galactosidase positive population (Fig. 6f; Extended Data Table 1) and p21 expression (Fig. 6g) in different KRAS mutant cancer cells with intact endogenous PKCα (PANC-1 cell) or with restored expression of PKCα (MIA PaCa2). Furthermore, knocking down PTPN14 rescued the inhibited colony formation ability of KRAS mutant cancer cells caused by activated PKCα (Fig. 6h). These data suggest that PTPN14 is a downstream mediator of PKCα-induced tumor suppression in KRAS mutant cancers.

CAMTA1 is a bio-indicator of PKCα/KRAS/CaM axis. Based on the data above, phosphorylation of KRAS by PKCα releases active CaM from the KRAS-CaM complex into the cytosol, sequentially modulating a broad range of cellular functional outputs, including cellular senescence. Some have reported that CaM and certain CaM-dependent signaling pathways positively regulate senescence programs in plant cells (Dai et al., 2018; Nie et al., 2012; Yang and Poovaiah, 2000). In particular, the CaM binding transcription activators (CAMTAs) are a group of transcription factors that act as target proteins of CaM and are widely conserved across eukaryotes. In plants, the CAMTAs function significantly in growth and development, defenses against biotic stress, and senescence in the response to abiotic stresses. Here, our nucleus extraction followed by western blotting analysis revealed that, between the two CAMTA proteins encoded in mammals, CAMTA-1 was less localized in the nuclear fraction from the cells transformed by KRAS-G12V when compared to the ones expressing HRAS-G12V or KRAS-G12V-S181D mutant, which are incapable of CaM binding (Extended Data Fig. 6i, left panel). Overexpression of PKCα increased both CAMTA proteins in the nuclear fraction of MIA PaCa-2 cells (Extended Data Fig. 6i, middle panel). Prostratin treatment reinforced the expression of CAMTA-1 in the nuclei of PANC-1 cells, whereas the combination of Trametinib and Palbociclib that induces cellular senescence through co-inhibition of CDK4/6 and MEK did not bring the same effect (Extended Data Fig. 6i, right panel). This result indicates that the increase of nucleus-localized CAMTA-

1 is specific to the cells with activated PKCα. Notably, in the Lrig1-Cre/ER/LSL/KRAS-G12D mice where tamoxifen-inducible Cre recombinase initiates the expression of KRAS-G12D and consequential formation of papilloma during wound-healing (Wang et al., 2015), administrating therapeutic level of prostratin not only prevented the tumor initiation (Wang et al., 2015) but also significantly elevated the expression level of nucleus-localized CAMTA-1 if the tumors formed (Extended Data Fig. 6j), thus validating that CAMTA-1, as a CaM responder, can be potentially used as a biomarker to indicate the anti-KRAS therapeutic efficacy of PKCα agonist *in vivo*.

Activation of PKCα induces a secretory phenotype in KRAS mutant tumor cells. Senescent cells are trapped in a prolonged growth arrest yet remain metabolically viable and biologically active through secretion of various cytokines and chemokines, also known as senescence-associated secretory phenotypes (SASPs) (Coppe et al., 2010). SASPs reportedly have physiological and pathological roles in aging-related diseases and cancers (Cuollo et al., 2020). We then evaluated the secretory proteins generated by the KRAS mutant cells undergoing active PKCα-induced senescence. Analysis of an antibody array, which detects 36 different human cytokines or chemokines, revealed that the expression of constitutively active PKCα elevated the generation of multiple secretory proteins in KRAS mutant pancreatic cancer cells (Fig. 7a). Among the analyzed cytokines or chemokines, the expressions of CCL3/4 (MIP-1α/-1β) and CXCL-1 were consistently changed (fold change in intensity was greater than 3) across two different cell lines upon genetic activation of PKCα (Fig. 7a). The expressions of the same chemokines were also increased in the cells treated with prostratin when compared to the senescence-inducing treatment with Trametinib and Palbociclib (Extended Data Fig. 7a), indicating that CCL3/4 (MIP-1α/-1β) and CXCL-1 might constitute the unique SASP caused by the activation of PKCα in KRAS mutant tumor cells. ELISA confirmed that, upon genetic or pharmacological activation of PKCα, different lung and pancreatic cancer cells harboring mutant KRAS produced and secreted CXCL1 to the culture media when compared to the control cells (Fig 7b; Extended Data Fig. 7b). Notably, the increased expression of *CXCL1* caused by activated PKCα occurred early at the transcriptional level, and inhibition of CaM activity by W7 treatment or knockdown of PTPN14 suppressed the increase in *CXCL1*

expression in the KRAS mutant tumor cells upon PKCα activation (Extended Data Fig. 7c-d). In addition, blocking the activity of CXCL1 by neutralizing antibody (Fig. 7b) partially rescued the growth inhibition caused by activated PKCα in KRAS mutant tumor cells (Fig. 7c; Extended Fig. 7g). Despite being non-detectable or low as the secreted forms in some cells (i.e. PANC-1 and NCI-H647), CCL3 and CCL4 were highly secreted from Panc02.13 cells with activation of PKCα (Extended Data Fig. 7e-f). In Panc02.13 cells, neutralizing the activity of CCL3 or CCL4 by antibodies (Fig. 7c, right panel) brought the similar rescued effect as neutralization of CXCL1 (Fig. 7c, left panel). These results suggest that the production of MIP-1α, -1β and/or CXCL-1 can be a SASP specific to the KRAS mutant tumor cells undergoing senescence induced by altered PKCα-KRAS-CaM signaling axis, which contributes to the growth inhibition caused by PKCα-induced senescence.

In summary, we discovered that the potential of prostratin to suppress oncogenic KRAS-mediated malignancies cannot be reproduced by other non-tumor-promoting PKC activators, byrostatin- I and -II. This specificity is mediated through the activation of PKCα, which exclusively phosphorylates KRAS at serine 181. Consequently, PKCα acts as a tumor suppressor in the cellular context of mutant KRAS, and, instead of promoting cell death, the activation of PKCα induces senescence through an elevated p21 expression, dependent on PTPN14. The nucleus-localized CAMTA1, a CaM dependent transcription factor, can be used as a biomarker to indicate the activation of PKCα, which disrupts KRAS-CaM axis and increases the level of cytosolic CaM. The KRAS mutant cells undergoing active PKCα-induced senescence exhibit a unique secretory phenotype, specifically an increased production of CCL3/4 and/or CXCL1, whose activity partially mediates the growth inhibition caused by active PKCα. Our results suggest that specific activation of PKCα can be an alternative strategy to target overall oncogenic KRAS-driven human cancers.

DISCUSSION

Throughout the development of KRAS inhibitors, including the breakthrough G12C inhibitors, most RAS research has focused on genetic or pharmacological disruption of KRAS activity through its G

domain, which functionally regulates the molecular GTP/GDP switches, and which contains RAS mutation hotspots. The G domains of all the three cancer-associated RAS isoforms are similar, and only the flexible C-terminal HVR can distinguish KRAS from other RAS isoforms. However, whether the HVR domain dictates the oncogenic outputs of KRAS remains incompletely explored. Consistent with our previous report that the binding of KRAS to CaM through serine 181 located in the HVR determines the specific downstream KRAS signaling pathway and CSC-like properties (Wang et al., 2015), our results here further reveal the specific regulatory mechanism of KRAS phosphorylation resulting in KRAS-CaM dissociation. Our findings significantly contribute to the knowledge of regulating KRAS activity through its HVR domain and can subsequently be used to drive the development of a novel and selective inhibitor of KRAS, which is urgently needed to treat patients suffering from malignancies driven by oncogenic KRAS. Since this inhibitory mechanism functions by targeting the HVR domain of KRAS, such inhibitors while being extremely selective towards KRAS, will not display a narrow range of efficacy against a specific mutant form of KRAS.

The HVR domain of KRAS contains a polybasic region that harbors three potential phosphorylation sites. Among these regions, serine 181 has been shown to be phosphorylated by PKC (Bivona et al., 2006). Coupled with our previous study, our findings here show that a non-tumor-promoting PKC modulator, prostratin, can specifically block the interaction of KRAS and CaM through activation of PKCα and phosphorylation of KRAS at serine 181. Mark Philips and colleagues proposed a similar concept for the use of PKC agonists, which stimulate phosphorylation of KRAS at serine 181, as a therapeutic approach to treat KRAS-dependent tumors (Bivona et al., 2006). In their study, treatment with bryostatin I at 1 μM led to phosphorylation of KRAS, and induced apoptosis in NIH\3T3 cells transformed with oncogenic KRAS through rapid dissociation of KRAS from the plasma membrane (Bivona et al., 2006). On the contrary, we did not observe subcellular translocation of the KRAS protein or apoptosis induced by treatment with prostratin or bryostatin in tumor cells harboring mutant KRAS. Notably, all PKC-C1 domain agonists exhibit a biphasic dose-dependent effect on activating PKC(Kedei et al., 2014) with maximal activation achieved at 10 nM for Bryostatin I (Ly et al., 2020; Matthews et al.,

1997). Thus, the effects induced by a high concentration (1 μM) of bryostatin I in KRAS-dependent tumor cells may not be specifically caused by the activation of PKC isozymes.

Additionally, non-tumor-promoting PKC modulators, including bryostatin I, have shown significant growth-inhibitory activity against various cancer cell lines *in vitro* and *in vivo* (Kraft et al., 1996; Pettit et al., 1996; Szallasi et al., 1996; Zonder et al., 2001). Bryostatin family compounds have therefore been examined in phase I and II studies using a wide range of tumor types. However, the results of several phase II studies using bryostatin I alone were disappointing in multiple types of cancers, including colon cancer, of which 30% - 40% carry a KRAS mutation (Mackay and Twelves, 2007; Marengo et al., 2011). The unsatisfactory clinical results may be caused by the inconsistent oncogenic or tumor-suppressive roles of PKC isozymes across human cancers. Moreover, we suggest here that prostratin but not bryostatin I/II has antitumor activity specifically in cancer cells expressing mutant KRAS, indicating that the clinical applicability of PKC activators as anticancer agents is likely context-specific (i.e., based on the tumor type and driver genetic alterations). Indeed, our results in this study reveal a tumor-suppressive role of PKCα in KRAS mutant cancer cells.

PKC isozymes regulate diverse cellular events, including cell proliferation and protein secretion. In addition, PKC isozymes function in immune cells and further modulate both innate and adaptive immunity. Different PKC isozymes are expressed in and act on various immune cells, such as T cells, B cells, and macrophages (Lim et al., 2015). Broad-spectrum PKC activators can therefore cause transient inflammation and rapid release of cytokines (cytokine storm) in the host. Such a drastic immune response can compromise the clinical applicability of PKC activators as anticancer agents. We found that PKCα but not other PKC isozymes specifically phosphorylates KRAS and consequently inhibits KRAS-driven malignancies. Activating or restoring the function of PKCα can be a novel therapeutic avenue for treating cancers driven by oncogenic KRAS with reduced systemic toxicity.

The discovery in the 1980s that PKC is a receptor for the tumor-promoting phorbol esters fueled the dogma that PKC is an oncoprotein (Garg et al., 2014; Kikkawa et al., 1983). Yet, years of clinical trials for cancer using PKC inhibitors not only failed, but in some instances worsened patient outcome.

The recent analysis of cancer-associated mutations in the PKC kinase family from diverse cancers revealed that PKC isozymes are generally inactivated in cancer, supporting a tumor suppressive function. (Antal et al., 2015; Newton and Brognard, 2017). Indeed, prior reports have indicated the potential tumor suppressive role of different PKC isozymes, including PKCα, in some types of cancers. Kazanietz and colleagues reported that PKCα induces senescence in non-small cell lung cancer cells through upregulation of p21 by using two cancer cell lines, H358 and H441 (Oliva et al., 2008). Alan Fields and colleagues observed that, upon Cre induction, genetic depletion of PKCα worsens the overall survival rate in LSL-KRAS-G12D mice by the activation of the p38 MAPK-TGFβ signaling axis (Hill et al., 2014). Their findings have hinted towards a role of PKCα as a tumor suppressor. However, in the study from the Kazanietz group, the upregulation of p21 is a global effect of PMC, which is a potent agonist to activate PKC in an isozyme-unbiased manner. In addition, they suggest that PKCα shows such tumor-suppressive effect during the activation in the S phase, which should be universal to all cancer cells. More specifically, the tumor suppressive mechanism of PKCα from their results may not completely explain whether the tumor-suppressive role of PKCα is specific to KRAS mutant tumor cells. Our study here not only confirms PKCα as a tumor suppressor but also elucidates an alternative mechanism underlying the tumor suppressive effect of activated PKCα specifically in the cellular context of mutant KRAS.

Combining MEK inhibitors with downstream cyclin-dependent kinase 4 and 6 (CDK4/6) inhibitors simultaneously reduces MAPK-regulated cyclin D levels and directly targets CDK4 kinase activity (Ruscetti et al., 2018), which, in principle, imitates the initial phase of oncogene-induced senescence (OIS) triggered by activation of p16 (Serrano et al., 1997). Our results here indicate that genetic or pharmacological activation of PKCα can induce a senescence program through PTPN14, which could be differentiated from classical OIS through collective activation of p16. PTPN14 reportedly interacts with the pivotal effector of Hippo signaling pathway, YAP, and further inhibits its transcriptional function (Liu et al., 2013; Wilson et al., 2014). In addition, PTPN14-YAP signaling axis has been reported to be integral to p53-mediated tumor suppression in pancreatic cancer (Mello et al., 2017; Wilson et al., 2014),

potentially coordinating multiple cell fates, including senescence (Raj and Bam, 2019). Even though the mechanism underlying the regulation of PTPN14 by KRAS-CaM axis remains to be further clarified, Calmodulation database and meta-analysis predictor (Lu et al., 1998) predicts that PTPN14 has a CaM interacting motif (a.a 59-70 THYFGLWFLSKS) and likely to be a CaM binding protein, raising the possibility that the binding to CaM determines the function of PTPN14. While somatic mutation of KRAS contributes to numerous types of tumorigeneses, germ-line mutations of KRAS are associated with developmental disorders, including Noonan syndrome (Gremer et al., 2011). New avenues for therapeutic strategies to target oncogenic KRAS can therefore bring additional benefit to patients suffering from KRAS-driven RASopathies. Senescence has been speculated to be a possible contributor to certain complex pathophenotypes of RASopathies (Engler et al., 2021). To study the physiological roles of PKCα may shed a light on KRAS-driven RASopathies, and our study also provides an alternative approach to treat RASopathies by targeting KRAS through activation of PKCα.

To facilitate the use of PKCα agonists as an alternative anti-KRAS agent in the clinic, it is necessary to have a biomarker specifically indicating the activation of PKCα and/or the changes in the KRAS/CaM signaling axis. While the activity of PKCα can be determined by phosphorylation of a threonine residue within its activation loop (a-loop), PKCα shares a highly conserved amino acid sequence of a-loop with other two conventional PKC isozymes, PKC-β and -γ. The conserved region across different PKC isozymes increases the cross-reactivity of antibodies and challenges the applicability of using phosphorylated PKCα in the a-loop as a specific biomarker. Our data here suggest that a CaM-dependent transcription activator, CAMTA-1, is stabilized and translocated to cell nucleus in the response to the KRAS-CaM dissociation and, therefore, could be a novel marker to indicate the therapeutic efficacy of PKCα agonists. CAMTAs are highly conserved proteins, are expressed broadly in the nervous system and upon depletion confer pleiotropic behavioral defects in flies, mice, and humans (Vuong-Brender et al., 2021). In addition, CAMTA1 reportedly functions as tumor suppressor to reduce the CSC-like properties in glioblastoma (Schraivogel et al., 2011). Even though we found that CAMTA1 is not directly involved in the PKCα-mediated senescence program reported here (data not

shown), the nuclear translocation of CAMTA1 induced by PKCα-KRAS-CaM signaling axis might be involved in regulation of some other oncogenic functions of KRAS, such as CSC-like properties or rare cases of neurodevelopmental disorders associated with KRAS mutation (Ryu et al., 2020).

In sum, our findings here can provide a clearer understanding of the physiological roles of PKCα in the development of oncogenic-KRAS driven malignancies and lay the groundwork to develop a new class of anti-KRAS treatments, potentially delivering a broad impact to not only treating cancers but also other diseases associated with KRAS mutation.

METHODS

Cell Lines

All human cancer cell lines were purchased from ATCC and maintained in appropriate culture media at 37°C and 5% CO_2. PANC-1 cells were maintained in Dulbecco's Eagles modified medium supplemented with 10% fetal bovine serum (FBS); other cell lines were maintained in ATCC-modified Roswell Park Memorial Institute (RPMI)-1640 medium. The medium was supplemented with 15% fetal bovine serum (FBS) and recombinant human insulin (Gibco 12585-014) for pancreatic cancer cells and with 10% FBS for both human lung and colon cancer cells. NIH\3T3 cells were originally purchased from ATCC. Ras-G12V-transformed NIH\3T3 cells were generated as previously described and maintained in Dulbecco's modified Eagle's medium (DMEM) supplemented with 10% FBS. Rasless MEFs(Drosten et al., 2010) were gifts from the NCI RAS Initiative. KP1233 (a murine KRAS-G12D-driven NSCLC cell line) was a gift from Dr Tyler Jack's laboratory at the Massachusetts institute of Technology (MIT) and were grown in RPMI-1640 medium supplemented with 10% FBS. The mouse pancreatic cancer cell line iKRAS* (Collins et al., 2012) was grown in DMEM supplemented with 10% FBS. The human pancreatic epithelial cell line was purchased from Cell Biologics (Cat. No. H6037) and cultured in a complete human epithelial cell medium (Cat. No. H6621).

Reagents and Antibodies

Prostratin (CAS 60857-08-1) was purchased from Santa Cruz Biotechnology (Cat. No. sc-203422A). Bryostatin I (Cat. No. 2383), bryostatin II (Cat. No. 5237), and PMA (Cat. No. 1201) were obtained from TOCRIS. Trametinib (S2673) and palbociclib (S1116) were purchased from Selleck Chemicals. The following antibodies were used for western blot analysis or staining in this study: anti-caspase3 (Cell Signaling #9662); anti-cleaved caspase 3 (Cell Signaling #9664); anti-PARP-1 (Cell Signaling #9532); anti-p21 (Cell Signaling #2947); anti-Lamin B1 (Cell Signaling #13435); anti-phospho-CaMKII (Thr286) (Cell Signaling #12716) (Abcam #ab5683); anti-phospho-p44/42 MAPK (Erk1/2) (Cell Signaling #4370); anti-p44/42 MAPK (Erk1/2) (Cell Signaling #4696); anti-KRAS (Sigma #WH0003845M1); anti-β-actin (Sigma #A2228); anti-PKCα (Santa Cruz #sc-8393); anti-CD44 (Santa Cruz #sc-7297); anti-PKCδ (Abcam #ab182126); anti-sox9 (Abcam #ab185966); anti-calmodulin (Abcam #ab45689); anti-HA (Invitrogen #26183 and #PA1-985); anti-pan-RAS (ThermoFisher #MA1-012); anti-phosphoserine (Enzo #ALX-850-023-KI01); anti-CAMTA-1 (ThermoFisher #PA5-103686); anti-CAMTA-2 (ThermoFisher # PA5-103687); anti-PTPN14 (Cell Signaling #13808). The secondary antibodies used for immunofluorescence staining were obtained from Invitrogen (#A32731 and A32723); the secondary antibodies used for western blot analysis were obtained from LI-COR (IRDye® 800CW Goat anti-Rabbit IgG Secondary Antibody and IRDye® 680RD Goat Anti-Mouse IgG Secondary Antibody) and Sigma (HRP anti- Rabbit or anti-Mouse Secondary antibodies). The constitutively active PKC mutant expression plasmid (PKC alpha CAT) was a gift from Bernard Weinstein (Addgene plasmid # 21234; http://n2t.net/Addgene:21234; RRID: Addgene_21234). siRNAs (pool) used for knocking down mouse CAMTA-1 were purchased from Horizon (ON-TARGETplus Mouse CAMTA1 siRNA; # L-051054-00-0005), and lipofectamine RNAiMAX reagent (ThermoFisher) was used to transfect siRNA into the target tumor cells. Antibodies used for neutralizing the activity of indicated chemokines are: Human CCL3/MIP-1 alpha Antibody (R&D # AF-270-NA); Human CCL4/MIP-1 beta Antibody (R&D # MAB271-100); and Human CXCL1 Antibody (R&D # MAB275-100).

Western Blot Analysis

Experimental cells were washed twice in ice-cold phosphate-buffered saline (PBS), lysed in 1% Triton lysis buffer (25 μM Tris [pH 7.5], 150 μM NaCl, 1% Triton X-100, 1 μM EDTA, 1 μM EGTA, 20 μM NaF, 1 μM Na_2VO_4, and 1 μM DTT) supplemented with a protease inhibitor cocktail (Roche) and cleared by centrifugation. Protein concentrations were determined by the Bio-Rad Protein Assay (Bio-Rad). Equal amounts of protein extracts were resolved by SDS-PAGE (NuPAGE; Invitrogen), and proteins were transferred to a nitrocellulose membrane. The membrane was immunoblotted with the indicated primary antibodies, incubated with secondary antibodies (details above), and were either visualized with a LI-COR Odyssey scanner or using Immobilon Western Chemiluminescent HRP Substrate (Sigma) and visualized by autoradiography.

2D CellTiter-Glo Assay

To measure the short-term effect of PKC activators on cell viability, 2000 cells were seeded in the wells of 96-well plates in a medium containing DMSO, prostratin, or bryostatin I/II as indicated for 72 hours. CellTiter-Glo® 2.0 reagent (Promega) was added and mixed by repeated pipetting. After incubation at room temperature for 20 min, luminescence was measured using a microplate reader. DMSO (the solvent) was used as the control. Relative cell viability was calculated as follows: (luminescence reading for PKC activator-treated cells)/(luminescence reading for DMSO-treated cells) X 100.

Sphere Formation Assay with Subsequent 3D CellTiter-Glo Assay

Cells were harvested, counted, and seeded into Ultra-Low Attachment Culture 96-well plates (Corning Life Science, Cat. No. 3261). One hundred cells were seeded in the wells of low-attachment 96-well plates in medium containing 10% Matrigel® (Corning). The seeded cells and formed spheres were maintained in complete serum containing medium. The medium was supplemented with various

PKC activators as indicated until spheres formed in 2-3 weeks. The formed spheres were observed twice weekly and counted one month after seeding.

To evaluate cell viability, an equal volume (100 µl) of CellTiter-Glo® 3D Cell Viability Assay reagent (Promega) was added and mixed by repeated pipetting to improve lysis of spheres. Plates were incubated for 30 min at room temperature while gently shaking on a rocker. Luminescence was measured using a microplate reader.

Crystal Violet Staining and Quantification

Cells were seeded in 24 well plates at $1X10^2$ cells per well in complete growth medium with indicated treatment with or without PKC activators. For the effects of constitutively active PKCα in cells, the cells were first seeded at same numbers in 6-well plates. The cells were then transfected with constitutively active PKCα expressing construct at indicated concentrations. 6 hours-post transfections, the cells were cultured back to complete growth medium. After visible colonies formed (usually on the 14th to 21st day depending on the cell line), they were visualized by staining with 0.05% crystal violet (in 0.1% methanol).

For further unbiased quantification of the density of cells adhering to the stained multiwell culture dishes, 1% SDS (300 µl per well of the 24-well plate) was then added to solubilize the stain. The plates were incubated with shaking at room temperature for 30 min or until the color was uniform with no areas of dense coloration in the bottom of the wells. The absorbance of each well was measured at 570 nm.

CETSA

The CETSA was performed as previously described (Jafari et al., 2014). In brief, PANC-1 and Panc02.13 cells were treated with the indicated treatments DMSO, prostratin (2 µM), and bryostatin II (0.5 nM) and indicated durations. After treatment, equal numbers of cells were aliquoted in 50 µl of 1X PBS containing a protease inhibitor cocktail in PCR tubes. Using the temperature gradient feature of

the thermal cycler, the cell aliquots were treated in parallel at different temperatures as indicated for 3 min. After incubation, another 50 µl of 1X PBS containing protease inhibitors was added, and the cells were lysed by three freeze-thaw cycles (flash freezing followed by thawing at 23°C and vortexing). After lysis, the lysates were centrifuged at 20,000 X g for 20 min at 4°C to remove the insoluble fraction. The soluble fraction was retained, mixed with NuPage™ LDS sample buffer (Thermo Fisher Scientific), and analyzed by western blotting.

RBD Pulldown Assay

The RAS pulldown assay was performed using an active Ras pulldown detection kit (Thermo Fisher Scientific) in accordance with the manufacturer's instructions. In brief, cells were lysed using lysis/binding/wash buffer. Glutathione resin was added to spin cups and precleaned with lysis/binding/wash buffer. The lysates were normalized to obtain equal amounts of total protein between samples. The normalized lysates were incubated with glutathione resin and 80 µg of GST-Raf1-RBD for 1 hour at 4°C with gentle shaking. After incubation, the resin was washed with lysis/binding/wash buffer. Finally, proteins bound to the resin were solubilized in a 2X reducing sample buffer, eluted by centrifugation, and analyzed by Western blotting.

CaM Pulldown Assay

Cells were washed twice in ice-cold PBS and lysed in 1% TX100-TNM lysis buffer (20 µM Tris [pH 7.5], 5 µM MgCl2, 150 µM NaCl, and 1% Triton X-100) supplemented with 1 µM DTT, 1 µM CaCl2, and protease and phosphatase inhibitors (Sigma-Aldrich). Equal amounts of protein from each sample were added to 50 µl of precleaned CaM binding beads (GE Healthcare, 17-0529-01) in 300 to 500 µl of 1% TX100-TNM lysis buffer and incubated with rotation at 4°C overnight (16-18 hours). The beads were washed 3 times with 1 ml of cold lysis buffer and boiled in NuPage™ LDS sample buffer (ThermoFisher

Scientific) to elute the bound proteins. Total cell lysates and pulldown samples were analyzed by Western blotting.

Senescence-Associated β-Galactosidase Staining

Cells were treated with prostratin or other compounds as indicated for 7 days to completely induce senescence. To evaluate b-galactosidase activity, cells were stained with a Senescence Cells Histochemical Staining Kit (Sigma, Cat. No. CS0030). The assays were performed following the manufacturer's instructions. To quantify the population of senescent cells, the CellEvent Senescence Green Flow Cytometry Assay Kit was used to detect cellular senescence via β-galactosidase hydrolysis (ThermoFisher, Cat. No. C10840) as per the manufacturer's instructions. After staining the cells were analyzed on the BD Fortessa flow cytometer to detect green probe fluorogenic signal. Flow data obtained from the cytometer was further analyzed using FlowJo software..

Cell Fractionation Assay

Cells were treated with the indicated compounds for indicated duration. After treatment, cells were washed in cold 1X PBS and harvested by scraping in a solution of 1X PBS + 1 mM EDTA. The cell pellets were resuspended in the hypotonic buffer (10 mM Tris-HCl, 1 mM EDTA, and 1 mM DTT supplemented with protease and phosphatase inhibitors). After incubation on ice in hypotonic buffer for 20 min, cells were lysed by repeated passage through a syringe with a 25-gauge 1/2-inch needle. The pellet (nuclear fraction) was isolated by centrifugation at 4°C and 2200 RPM for 3 min. The supernatant was removed and centrifuged at 10,000 RPM for 15 min at 4°C to collect the pellet (crude membrane fraction) and supernatant (crude cytoplasmic fraction). The membrane fraction pellet was washed three times with hypotonic buffer and centrifuged at 10,000 RPM for 10 min at 4°C. The final pellet was resuspended in Western lysis buffer. Membrane contamination from the crude cytoplasmic fraction was removed by centrifugation at 45,000 RPM for 30 min at 4°C using a Sorvall Discovery M120 SE ultracentrifuge with an S120AT2 rotor. The total protein lysates and the membrane and cytoplasmic

protein fractions were mixed with NuPage™ LDS sample buffer (Thermo Fisher Scientific) and analyzed by western blotting. For the nucleus extraction assay, the cells were first transfected with constitutively active PKCα expressing constructs. 48 hours post-transfection, the cellular nucleus was extracted by using Nuclear Extraction Kit (ab113474, Abcam) in accordance with the manufacturer's instructions.

PKC Kinase Activity Assay

To measure the working concentration of prostratin or bryostatin required for pan-PKC activation in cancer cells and for use in the functional assays, cells were first treated with compounds as indicated for at least 24 hours. The PKC isoform activities were examined using a PKC enzyme activity kit (Abcam #139437). In brief, cells were washed twice in ice-cold PBS and lysed on ice for 10 min. Then, the lysates were centrifuged at 13,000 RPM for 15 min, and the clear supernatants were analyzed for kinase activity according to the manufacturer's protocol. Finally, the absorbance of the microplate wells was measured in a spectrophotometer at 450 nm.

Immunoprecipitation

To test whether KRAS acts as a PKC substrate upon stimulation with prostratin or co-transfection of PKCα and oncogenic RAS expressing constructs as indicated, cells were washed 3× with 37°C Hank's balanced salt solution (HBSS), and the indicated drugs were then added for 30 min in a 37°C non-CO_2 incubator. Cells were subsequently lysed (1 mM NaF, 1 mM Na_3VO_4, 10 nM calyculin A, 1 mM PMSF, 1 mg complete EDTA-free protease inhibitor cocktail [Roche] in RIPA buffer), scraped, collected, and centrifuged at 15,000 X *g* for 30 min at 4°C. The supernatant was collected and incubated with an immunoprecipitating antibody targeting phospho-(Ser) PKC substrates (#2261, Cell Signaling) or HA tag (#71-5500, Invitrogen) for 16–24 hours at 4°C. The lysate-antibody mix was incubated for 3 hours with Protein A/G PLUS-Agarose beads (Santa Cruz) pre-equilibrated in RIPA buffer. After four washes with ice-cold Dulbecco's phosphate-buffered saline (DPBS), bound protein was eluted by boiling for 10

minutes in NuPage™ LDS sample buffer. Whole-cell lysates, supernatants, and immunoprecipitated samples were subjected to western blotting with an antibody against KRAS (Clone 3B10-2F2, Sigma, # WH0003845M1), Pan-RAS (#MA1-012, Invitrogen), and HA tag (#26183, Invitrogen).

Immunofluorescence Staining

Cells were first grown on cover glasses in 24-well plates. After attachment, the cells were treated with PKC activators as indicated for 24 hours. Prior to staining, the cells were washed briefly with 1X PBS, fixed with 4% paraformaldehyde for 15 min, and incubated for 1 min in a solution of 0.01% Triton X-100 in PBS. The cells were then washed three times with 1X PBS and blocked in 1% BSA for 10 min at room temperature. The cells were then incubated with primary antibodies in 1% BSA overnight at 4°C with gentle shaking. Before incubation with secondary antibodies in 1% BSA for 40 min at room temperature in the dark, the cells were washed three times with 1X PBS. The stained cells were counterstained, fixed with ProLong Gold Antifade Mountant with the blue DNA stain DAPI (Thermo Fisher #P36931), and mounted on microscope slides.

Genome-Wide CRISPR/Cas9 Knockout Screens

In this study, the Human GeCKOv2A CRISPR knockout pooled library was used to identify genes responsible for prostratin resistance in PANC-1 cells. The library was obtained from Addgene (73178-LV). In brief, we first established a stable Cas9-expressing PANC-1 cell line by lentiviral transduction of the Cas9 coding sequence. The transduced cells were selected with 2.0 μg/ml puromycin for 7 days to generate a mutant cell pool, which was then treated with vehicle (DMSO) or prostratin (4 μM) for 21 days. After treatment, at least 3×10^7 cells were collected for genomic DNA (gDNA) extraction to ensure greater than 400X coverage of the GeCKO v2A library. The sgRNA sequences were amplified using NEBNext® High-Fidelity 2X PCR Master Mix and subjected to massive parallel amplicon sequencing carried out by the UPMC Genome Core. Sequencing data from the Cas9 screen were analyzed using MAGeCK (V0.5.9.4, Li et al., 2014) (Li et al., 2014) with the “test” option and default settings. Two

replicates of untreated and treated conditions were compared, and the “combined gene summary" output, which uses information from the 4 sgRNAs in the library for each gene, was used to compute a per-gene score.

Establishment of Cell Lines with CRISPR/Cas9-Mediated Gene Knockout

Cancer cell lines with PKCα knockout were established following a previously described protocol (Ran et al., 2013). The sequences of the forward/reverse primers for generating PRKCA gDNA were as follows: For1- AGGAAGGAAACATGGAACTC; Rev1- GAGTTCCATGTTTCCTTCCT; For2- CCTTGACCGAGTGAAACTCA; Rev2- TGAGTTTCACTCGGTCAAGG; For3- GCTCCACACTAAATCCGCAG; and Rev3- CTGCGGATTTAGTGTGGAGC. Western blot analysis was used to confirm knockout. At least two different knockout clones were selected for experiments. Cells with Cas9 expression but without knockout were used as control cells.

Re-expression of PKCα

Cancer cells with PKCα knockout or lacking endogenous expression of PKCα were infected with a lentiviral vector carrying human PRKCA cDNA ORF (Horizon Discovery, # OHS5899-202625016). The infected cells were selected in blasticidin (10 μg/mL) containing complete medium for at least two weeks. The re-stored expression of PKCα in the pool of cells post-selection was confirmed by western blot analysis.

For the expression of HA-tagged PKCα, the cells were transfected with pHAGE-PKCα-WT, -CAT, or -DN, which were gifts from Dr. Bernard Weinstein (Addgene plasmid # 21232; http://n2t.net/addgene:21232; RRID:Addgene_21232; Addgene plasmid # 21234; http://n2t.net/addgene:21234; RRID:Addgene_21234; Addgene plasmid # 21235; http://n2t.net/addgene:21235; RRID:Addgene_21235, respectively) by using Lipofectamine 3000

(Invitrogen). The ectopic expression of PKCα was confirmed by western blotting and probing for the HA-tag.

Tumor xenografts

All experiments were approved by the IACUC of the University of Pittsburgh. Human pancreatic cancer cells were subcutaneously injected into nude mice (Nu/Nu) at 0.1×10^6 cells per flank. Palpable tumors were measured once a week. The animals were divided into at least five mice per group. Mice bearing tumors derived from MIA PaCa2 were monitored for one month (two months for mice bearing PANC-1-derived tumors) and euthanized when distressed. All studies were conducted in accordance with the Institutional Animal Care and Use Committee, and all relevant ethical regulations were followed. Equal numbers of female and male mice were used in the study.

Detection of active calmodulin in the cytosolic fraction

Cells were first transfected with cytosol-targeted FRET biosensor, which was a gift from Jin Zhang (Addgene plasmid # 64729; http://n2t.net/addgene:64729; RRID:Addgene_64729). The cells were treated with PKC activators 24 hours post-transfection, and the reading of YPet was detected and quantified by using Synergy LX Multi-Mode Reader (BioTak) at different timepoints. To measure the effect of PKCα expression in the cytosolic distribution of CaM, the cells were co-transfected with pcDNA3-Cyto-CaNAR2 and indicated pHAGE-PKCα construct at 1:1 ratio. YPet signal was measured at 48th hour post-transfection, and the numbers of viable cells defined by CellTiter Glo were used for normalization.

Quantitative PCR

Total RNAs were isolated and purified with the QIAGEN RNAeasy kit; 1 μg RNA per specimen was reverse-transcribed into cDNA with the SuperScript™ First-Strand Synthesis System for RT-PCR (Invitrogen). Possible contamination of genomic DNA was excluded by treatments of DNase I.

Quantitative real-time PCR array analysis was performed with SYBR Green (Applied Biosystem). Fold differences and statistical analyses were calculated with the GraphPad Prism 4.00 for Windows (GraphPad Software). The oligo sequences used to detect human CDKN1A are: forward 5' TGTCCGTCAGAACCCATGC 3' and reverse 5' AAAGTCGAAGTTCCATCGCTC 3'.

Human Cytokine Antibody Array

The proteome profiler Human cytokine array kit (R&D #ARY005B) was used to detect the level of 36 different cytokines from total cell protein lysates after indicated treatments. The array staining was performed as per the manufacturer's instructions and resultant autoradiographic films were scanned and analyzed with ImageJ to detect and quantify the intensity of each individual cytokine spot.

Human CCL3, CCL4, and CXCL1 ELISA

Human CCL3/MIP-1 alpha Quantikine ELISA Kit (R&D # DMA00); Human MIP1 beta ELISA Kit (CCL4) (abcam #ab100597); and Human CXCL1 ELISA Kit (GRO alpha) (abcam #ab190805) were used to detect the indicated chemokines. The assays were performed following the manufacturer's instructions. To collect the culture supernatant for ELISA, the tumor cells were first treated with 2 μM prostratin or transfected with constitutively active mutant of PKCα. 96 hours post-treatment or transfection, the cell culture supernatant was collected and centrifuged at 3,000 rpm to remove the cell debris. Freshly collected cell-free supernatant was then subjected to ELISA. Each experiment was repeated independently for at least 3 times to get the mean values. The supernatant collected from cells treated with DMSO or transfected with empty vector were used as control.

Statistical Analysis

Experiments were repeated at least three times when appropriate. Each independent experiment was performed with at least four technical replicates. Data are presented as the mean ± standard error

of the mean values. All error bars in these assays indicate the standard deviation (s.d.) of four to eight technical replicates unless noted otherwise. Prism 7.0 software (GraphPad Software Inc.) was used for all statistical analyses, and P values < 0.05 were considered statistically significant. Paired or unpaired t tests were used for comparisons between two groups where appropriate.

Acknowledgements

This work is generously supported by UPMC Hillman Cancer Center Internal Startup funding (M-T Wang) and partially supported by award number R21CA259457 (Y.N.G).

References

Althubiti, M., Lezina, L., Carrera, S., Jukes-Jones, R., Giblett, S.M., Antonov, A., Barlev, N., Saldanha, G.S., Pritchard, C.A., Cain, K., *et al.* (2014). Characterization of novel markers of senescence and their prognostic potential in cancer. Cell Death Dis *5*, e1528.

Alvarez-Moya, B., Lopez-Alcala, C., Drosten, M., Bachs, O., and Agell, N. (2010). K-Ras4B phosphorylation at Ser181 is inhibited by calmodulin and modulates K-Ras activity and function. Oncogene *29*, 5911-5922.

Antal, C.E., Hudson, A.M., Kang, E., Zanca, C., Wirth, C., Stephenson, N.L., Trotter, E.W., Gallegos, L.L., Miller, C.J., Furnari, F.B., *et al.* (2015). Cancer-associated protein kinase C mutations reveal kinase's role as tumor suppressor. Cell *160*, 489-502.

Ballester, R., Furth, M.E., and Rosen, O.M. (1987). Phorbol ester- and protein kinase C-mediated phosphorylation of the cellular Kirsten ras gene product. J Biol Chem *262*, 2688-2695.

Beans, E.J., Fournogerakis, D., Gauntlett, C., Heumann, L.V., Kramer, R., Marsden, M.D., Murray, D., Chun, T.W., Zack, J.A., and Wender, P.A. (2013). Highly potent, synthetically accessible prostratin analogs induce latent HIV expression in vitro and ex vivo. Proc Natl Acad Sci U S A *110*, 11698-11703.

Bivona, T.G., Quatela, S.E., Bodemann, B.O., Ahearn, I.M., Soskis, M.J., Mor, A., Miura, J., Wiener, H.H., Wright, L., Saba, S.G., *et al.* (2006). PKC regulates a farnesyl-electrostatic switch on K-Ras that promotes its association with Bcl-XL on mitochondria and induces apoptosis. Mol Cell *21*, 481-493.

Canon, J., Rex, K., Saiki, A.Y., Mohr, C., Cooke, K., Bagal, D., Gaida, K., Holt, T., Knutson, C.G., Koppada, N., *et al.* (2019). The clinical KRAS(G12C) inhibitor AMG 510 drives anti-tumour immunity. Nature *575*, 217-223.

Christin, J.R., Wang, C., Chung, C.Y., Liu, Y., Dravis, C., Tang, W., Oktay, M.H., Wahl, G.M., and Guo, W. (2020). Stem Cell Determinant SOX9 Promotes Lineage Plasticity and Progression in Basal-like Breast Cancer. Cell Rep *31*, 107742.

Collins, M.A., Bednar, F., Zhang, Y., Brisset, J.C., Galban, S., Galban, C.J., Rakshit, S., Flannagan, K.S., Adsay, N.V., and Pasca di Magliano, M. (2012). Oncogenic Kras is required for both the initiation and maintenance of pancreatic cancer in mice. J Clin Invest *122*, 639-653.

Coppe, J.P., Desprez, P.Y., Krtolica, A., and Campisi, J. (2010). The senescence-associated secretory phenotype: the dark side of tumor suppression. Annu Rev Pathol *5*, 99-118.

Cox, A.D., and Der, C.J. (2002). Ras family signaling: therapeutic targeting. Cancer Biol Ther *1*, 599-606.

Cuollo, L., Antonangeli, F., Santoni, A., and Soriani, A. (2020). The Senescence-Associated Secretory Phenotype (SASP) in the Challenging Future of Cancer Therapy and Age-Related Diseases. Biology (Basel) *9*.

Dai, C., Lee, Y., Lee, I.C., Nam, H.G., and Kwak, J.M. (2018). Calmodulin 1 Regulates Senescence and ABA Response in Arabidopsis. Front Plant Sci *9*, 803.

Dogan, S., Shen, R., Ang, D.C., Johnson, M.L., D'Angelo, S.P., Paik, P.K., Brzostowski, E.B., Riely, G.J., Kris, M.G., Zakowski, M.F., *et al.* (2012). Molecular epidemiology of EGFR and KRAS mutations in 3,026 lung adenocarcinomas: higher susceptibility of women to smoking-related KRAS-mutant cancers. Clin Cancer Res *18*, 6169-6177.

Drosten, M., Dhawahir, A., Sum, E.Y., Urosevic, J., Lechuga, C.G., Esteban, L.M., Castellano, E., Guerra, C., Santos, E., and Barbacid, M. (2010). Genetic analysis of Ras signalling pathways in cell proliferation, migration and survival. EMBO J *29*, 1091-1104.

Engler, M., Fidan, M., Nandi, S., and Cirstea, I.C. (2021). Senescence in RASopathies, a possible novel contributor to a complex pathophenoype. Mech Ageing Dev *194*, 111411.

Fell, J.B., Fischer, J.P., Baer, B.R., Blake, J.F., Bouhana, K., Briere, D.M., Brown, K.D., Burgess, L.E., Burns, A.C., Burkard, M.R., *et al.* (2020). Identification of the Clinical Development Candidate MRTX849, a Covalent KRAS(G12C) Inhibitor for the Treatment of Cancer. J Med Chem *63*, 6679-6693.

Freund, A., Laberge, R.M., Demaria, M., and Campisi, J. (2012). Lamin B1 loss is a senescence-associated biomarker. Mol Biol Cell *23*, 2066-2075.

Garg, R., Benedetti, L.G., Abera, M.B., Wang, H., Abba, M., and Kazanietz, M.G. (2014). Protein kinase C and cancer: what we know and what we do not. Oncogene *33*, 5225-5237.

Gremer, L., Merbitz-Zahradnik, T., Dvorsky, R., Cirstea, I.C., Kratz, C.P., Zenker, M., Wittinghofer, A., and Ahmadian, M.R. (2011). Germline KRAS mutations cause aberrant

biochemical and physical properties leading to developmental disorders. Hum Mutat *32*, 33-43.
Hallin, J., Engstrom, L.D., Hargis, L., Calinisan, A., Aranda, R., Briere, D.M., Sudhakar, N., Bowcut, V., Baer, B.R., Ballard, J.A.*, et al.* (2020). The KRAS(G12C) Inhibitor MRTX849 Provides Insight toward Therapeutic Susceptibility of KRAS-Mutant Cancers in Mouse Models and Patients. Cancer Discov *10*, 54-71.
Hill, K.S., Erdogan, E., Khoor, A., Walsh, M.P., Leitges, M., Murray, N.R., and Fields, A.P. (2014). Protein kinase Calpha suppresses Kras-mediated lung tumor formation through activation of a p38 MAPK-TGFbeta signaling axis. Oncogene *33*, 2134-2144.
Hobbs, G.A., Wittinghofer, A., and Der, C.J. (2016). Selective Targeting of the KRAS G12C Mutant: Kicking KRAS When It's Down. Cancer Cell *29*, 251-253.
Jafari, R., Almqvist, H., Axelsson, H., Ignatushchenko, M., Lundback, T., Nordlund, P., and Martinez Molina, D. (2014). The cellular thermal shift assay for evaluating drug target interactions in cells. Nat Protoc *9*, 2100-2122.
Jiang, G., and Dandekar, S. (2015). Targeting NF-kappaB signaling with protein kinase C agonists as an emerging strategy for combating HIV latency. AIDS Res Hum Retroviruses *31*, 4-12.
Kapalczynska, M., Kolenda, T., Przybyla, W., Zajaczkowska, M., Teresiak, A., Filas, V., Ibbs, M., Blizniak, R., Luczewski, L., and Lamperska, K. (2018). 2D and 3D cell cultures - a comparison of different types of cancer cell cultures. Arch Med Sci *14*, 910-919.
Kedei, N., Chen, J.Q., Herrmann, M.A., Telek, A., Goldsmith, P.K., Petersen, M.E., Keck, G.E., and Blumberg, P.M. (2014). Molecular systems pharmacology: isoelectric focusing signature of protein kinase Cdelta provides an integrated measure of its modulation in response to ligands. J Med Chem *57*, 5356-5369.
Kolczynska, K., Loza-Valdes, A., Hawro, I., and Sumara, G. (2020). Diacylglycerol-evoked activation of PKC and PKD isoforms in regulation of glucose and lipid metabolism: a review. Lipids Health Dis *19*, 113.
Kraft, A.S., Woodley, S., Pettit, G.R., Gao, F., Coll, J.C., and Wagner, F. (1996). Comparison of the antitumor activity of bryostatins 1, 5, and 8. Cancer Chemother Pharmacol *37*, 271-278.
Li, W., Xu, H., Xiao, T., Cong, L., Love, M.I., Zhang, F., Irizarry, R.A., Liu, J.S., Brown, M., and Liu, X.S. (2014). MAGeCK enables robust identification of essential genes from genome-scale CRISPR/Cas9 knockout screens. Genome Biol *15*, 554.
Lim, P.S., Sutton, C.R., and Rao, S. (2015). Protein kinase C in the immune system: from signalling to chromatin regulation. Immunology *146*, 508-522.
Liu, X., Yang, N., Figel, S.A., Wilson, K.E., Morrison, C.D., Gelman, I.H., and Zhang, J. (2013). PTPN14 interacts with and negatively regulates the oncogenic function of YAP. Oncogene *32*, 1266-1273.

Lu, Z., Liu, D., Hornia, A., Devonish, W., Pagano, M., and Foster, D.A. (1998). Activation of protein kinase C triggers its ubiquitination and degradation. Mol Cell Biol *18*, 839-845.
Lucas, M., and Sanchez-Margalet, V. (1995). Protein kinase C involvement in apoptosis. Gen Pharmacol *26*, 881-887.
Ly, C., Shimizu, A.J., Vargas, M.V., Duim, W.C., Wender, P.A., and Olson, D.E. (2020). Bryostatin 1 Promotes Synaptogenesis and Reduces Dendritic Spine Density in Cortical Cultures through a PKC-Dependent Mechanism. ACS Chem Neurosci *11*, 1545-1554.
Lynn, F.C., Smith, S.B., Wilson, M.E., Yang, K.Y., Nekrep, N., and German, M.S. (2007). Sox9 coordinates a transcriptional network in pancreatic progenitor cells. Proc Natl Acad Sci U S A *104*, 10500-10505.
Mackay, H.J., and Twelves, C.J. (2007). Targeting the protein kinase C family: are we there yet? Nat Rev Cancer *7*, 554-562.
Marengo, B., De Ciucis, C., Ricciarelli, R., Pronzato, M.A., Marinari, U.M., and Domenicotti, C. (2011). Protein kinase C: an attractive target for cancer therapy. Cancers (Basel) *3*, 531-567.
Matthews, S.A., Pettit, G.R., and Rozengurt, E. (1997). Bryostatin 1 induces biphasic activation of protein kinase D in intact cells. J Biol Chem *272*, 20245-20250.
McCormick, F. (2015). KRAS as a Therapeutic Target. Clin Cancer Res *21*, 1797-1801.
McCormick, F. (2020). Sticking it to KRAS: Covalent Inhibitors Enter the Clinic. Cancer Cell *37*, 3-4.
Mehta, S., Aye-Han, N.N., Ganesan, A., Oldach, L., Gorshkov, K., and Zhang, J. (2014). Calmodulin-controlled spatial decoding of oscillatory Ca2+ signals by calcineurin. Elife *3*, e03765.
Mello, S.S., Valente, L.J., Raj, N., Seoane, J.A., Flowers, B.M., McClendon, J., Bieging-Rolett, K.T., Lee, J., Ivanochko, D., Kozak, M.M., *et al.* (2017). A p53 Super-tumor Suppressor Reveals a Tumor Suppressive p53-Ptpn14-Yap Axis in Pancreatic Cancer. Cancer Cell *32*, 460-473 e466.
Newton, A.C., and Brognard, J. (2017). Reversing the Paradigm: Protein Kinase C as a Tumor Suppressor. Trends Pharmacol Sci *38*, 438-447.
Nie, H., Zhao, C., Wu, G., Wu, Y., Chen, Y., and Tang, D. (2012). SR1, a calmodulin-binding transcription factor, modulates plant defense and ethylene-induced senescence by directly regulating NDR1 and EIN3. Plant Physiol *158*, 1847-1859.
Oliva, J.L., Caino, M.C., Senderowicz, A.M., and Kazanietz, M.G. (2008). S-Phase-specific activation of PKC alpha induces senescence in non-small cell lung cancer cells. J Biol Chem *283*, 5466-5476.
Pettit, G.R., Gao, F., Blumberg, P.M., Herald, C.L., Coll, J.C., Kamano, Y., Lewin, N.E., Schmidt, J.M., and Chapuis, J.C. (1996). Antineoplastic agents. 340. Isolation and structural elucidation of bryostatins 16-18. J Nat Prod *59*, 286-289.

Raj, N., and Bam, R. (2019). Reciprocal Crosstalk Between YAP1/Hippo Pathway and the p53 Family Proteins: Mechanisms and Outcomes in Cancer. Front Cell Dev Biol *7*, 159.

Ran, F.A., Hsu, P.D., Wright, J., Agarwala, V., Scott, D.A., and Zhang, F. (2013). Genome engineering using the CRISPR-Cas9 system. Nat Protoc *8*, 2281-2308.

Ruscetti, M., Leibold, J., Bott, M.J., Fennell, M., Kulick, A., Salgado, N.R., Chen, C.C., Ho, Y.J., Sanchez-Rivera, F.J., Feucht, J.*, et al.* (2018). NK cell-mediated cytotoxicity contributes to tumor control by a cytostatic drug combination. Science *362*, 1416-1422.

Ryan, M.B., Der, C.J., Wang-Gillam, A., and Cox, A.D. (2015). Targeting RAS-mutant cancers: is ERK the key? Trends Cancer *1*, 183-198.

Ryu, H.H., Kang, M., Hwang, K.D., Jang, H.B., Kim, S.J., and Lee, Y.S. (2020). Neuron type-specific expression of a mutant KRAS impairs hippocampal-dependent learning and memory. Sci Rep *10*, 17730.

Schraivogel, D., Weinmann, L., Beier, D., Tabatabai, G., Eichner, A., Zhu, J.Y., Anton, M., Sixt, M., Weller, M., Beier, C.P.*, et al.* (2011). CAMTA1 is a novel tumour suppressor regulated by miR-9/9* in glioblastoma stem cells. EMBO J *30*, 4309-4322.

Serrano, M., Lin, A.W., McCurrach, M.E., Beach, D., and Lowe, S.W. (1997). Oncogenic ras provokes premature cell senescence associated with accumulation of p53 and p16INK4a. Cell *88*, 593-602.

Seymour, P.A., Freude, K.K., Tran, M.N., Mayes, E.E., Jensen, J., Kist, R., Scherer, G., and Sander, M. (2007). SOX9 is required for maintenance of the pancreatic progenitor cell pool. Proc Natl Acad Sci U S A *104*, 1865-1870.

Sims, M.W., Winter, J., Brennan, S., Norman, R.I., Ng, G.A., Squire, I.B., and Rainbow, R.D. (2014). PKC-mediated toxicity of elevated glucose concentration on cardiomyocyte function. Am J Physiol Heart Circ Physiol *307*, H587-597.

Soh, J.W., and Weinstein, I.B. (2003). Roles of specific isoforms of protein kinase C in the transcriptional control of cyclin D1 and related genes. J Biol Chem *278*, 34709-34716.

Spitaler, M., and Cantrell, D.A. (2004). Protein kinase C and beyond. Nat Immunol *5*, 785-790.

Stinchcombe, T.E., and Der, C.J. (2011). Are all KRAS mutations created equal? Lancet Oncol *12*, 717-718.

Szallasi, Z., Du, L., Levine, R., Lewin, N.E., Nguyen, P.N., Williams, M.D., Pettit, G.R., and Blumberg, P.M. (1996). The bryostatins inhibit growth of B16/F10 melanoma cells in vitro through a protein kinase C-independent mechanism: dissociation of activities using 26-epi-bryostatin 1. Cancer Res *56*, 2105-2111.

von Burstin, V.A., Xiao, L., and Kazanietz, M.G. (2010). Bryostatin 1 inhibits phorbol ester-induced apoptosis in prostate cancer cells by differentially modulating protein kinase C (PKC) delta translocation and preventing PKCdelta-mediated release of tumor necrosis factor-alpha. Mol Pharmacol *78*, 325-332.

Vuong-Brender, T.T., Flynn, S., Vallis, Y., and de Bono, M. (2021). Neuronal calmodulin levels are controlled by CAMTA transcription factors. Elife *10*.

Wang, A.S., Ong, P.F., Chojnowski, A., Clavel, C., and Dreesen, O. (2017). Loss of lamin B1 is a biomarker to quantify cellular senescence in photoaged skin. Sci Rep *7*, 15678.

Wang, M.T., Holderfield, M., Galeas, J., Delrosario, R., To, M.D., Balmain, A., and McCormick, F. (2015). K-Ras Promotes Tumorigenicity through Suppression of Non-canonical Wnt Signaling. Cell *163*, 1237-1251.

Waters, A.M., and Der, C.J. (2018). KRAS: The Critical Driver and Therapeutic Target for Pancreatic Cancer. Cold Spring Harb Perspect Med *8*.

Wender, P.A., Baryza, J.L., Brenner, S.E., DeChristopher, B.A., Loy, B.A., Schrier, A.J., and Verma, V.A. (2011). Design, synthesis, and evaluation of potent bryostatin analogs that modulate PKC translocation selectivity. Proc Natl Acad Sci U S A *108*, 6721-6726.

Wender, P.A., Dechristopher, B.A., and Schrier, A.J. (2008). Efficient synthetic access to a new family of highly potent bryostatin analogues via a Prins-driven macrocyclization strategy. J Am Chem Soc *130*, 6658-6659.

Wilson, K.E., Li, Y.W., Yang, N., Shen, H., Orillion, A.R., and Zhang, J. (2014). PTPN14 forms a complex with Kibra and LATS1 proteins and negatively regulates the YAP oncogenic function. J Biol Chem *289*, 23693-23700.

Wu, R., Chen, H., Chang, N., Xu, Y., Jiao, J., and Zhang, H. (2020). Unlocking the Drug Potential of the Bryostatin Family: Recent Advances in Product Synthesis and Biomedical Applications. Chemistry *26*, 1166-1195.

Xue, J.Y., Zhao, Y., Aronowitz, J., Mai, T.T., Vides, A., Qeriqi, B., Kim, D., Li, C., de Stanchina, E., Mazutis, L.*, et al.* (2020). Rapid non-uniform adaptation to conformation-specific KRAS(G12C) inhibition. Nature *577*, 421-425.

Yang, T., and Poovaiah, B.W. (2000). An early ethylene up-regulated gene encoding a calmodulin-binding protein involved in plant senescence and death. J Biol Chem *275*, 38467-38473.

Zeitouni, D., Pylayeva-Gupta, Y., Der, C.J., and Bryant, K.L. (2016). KRAS Mutant Pancreatic Cancer: No Lone Path to an Effective Treatment. Cancers (Basel) *8*.

Zhao, Y., Murciano-Goroff, Y.R., Xue, J.Y., Ang, A., Lucas, J., Mai, T.T., Da Cruz Paula, A.F., Saiki, A.Y., Mohn, D., Achanta, P.*, et al.* (2021). Diverse alterations associated with resistance to KRAS(G12C) inhibition. Nature *599*, 679-683.

Zhu, T., Tsuji, T., and Chen, C. (2010). Roles of PKC isoforms in the induction of apoptosis elicited by aberrant Ras. Oncogene *29*, 1050-1061.

Zonder, J.A., Shields, A.F., Zalupski, M., Chaplen, R., Heilbrun, L.K., Arlauskas, P., and Philip, P.A. (2001). A phase II trial of bryostatin 1 in the treatment of metastatic colorectal cancer. Clin Cancer Res *7*, 38-42.

Legends

Fig 1. Prostratin but not bryostatin I or II suppresses the malignancy of transformed cells or cancer cells expressing mutant KRAS *in vitro*.

(a) Chemical structures of prostratin, bryostatin I, and bryostatin II.

(b) PKC enzyme activity assay using pan-PKC substrates to determine the working concentrations of prostratin, bryostatin I, and bryostatin II in two different human pancreatic cancer cell lines harboring mutant KRAS.

(c) Upon treatments, prostratin reduced the numbers of viable human cancer cells, whereas neither bryostatin I nor bryostatin II did not reduce numbers of viable cells when compared to DMSO treated control. The mutant forms of KRAS in each cell line are labeled as indicated. Cells were treated for 72 hours. A Cell Titer-Glo assay was used to determine cell viability, and the results were normalized to those in the control (DMSO-treated) group. (n=6; *** $P < 0.001$; **** $P < 0.0001$) Means are with s.d. values and plotted as bars with error bars.

(d) Colony formation assay followed by crystal violet staining (left panel) in NIH\3T3 cells transformed with different RAS mutants, in human pancreatic cancer cell lines, and in human lung cancer cells in response to prostratin, bryostatin I, or bryostatin II. The treatment concentrations are indicated. Cells were cultured in complete medium containing the compound until visible colonies formed. The crystal violet was dissolved, and the staining intensity was quantified by absorbance measurement (right panel). Prostratin but not bryostatin I or II blocked colony formation in NIH\3T3 cells transformed with KRAS-G12V and in cancer cell lines expressing mutant KRAS. NIH\3T3 cells expressing HRAS-G12V or KRAS-G12V-S181A maintained their colony-forming ability after prostratin treatment. The mutation status of each cell line is indicated, and the mutant forms of KRAS are labeled in bold font. Means of the absorbance at 570 nm with s.d. values (n=4) are plotted as bars with error bars. (* $P < 0.05$, ** $P < 0.01$)

(e) 3D sphere formation assay of a series of cancer cell lines harboring mutant KRAS and treated with prostratin, bryostatin I, or bryostatin II. Prostratin but not bryostatin I or II inhibited the sphere-forming ability of different human cancer cell lines. Representative images of a well containing spheres in a 96-well plate are shown in the left panel. In the representative images, cells were treated with 2 μM prostratin, 1 nM bryostatin I, or 0.5 nM bryostatin II. DMSO was used as the solvent control. A 3D Cell Titer-Glo assay was used to quantitatively determine the overall viability of spheres. (n=6; * $P < 0.05$, ** $P < 0.01$; *** $P < 0.001$) Means are with s.d. values and plotted as bars with error bars.

Fig 2. Prostratin induces phosphorylation of KRAS at serine 181, consequent KRAS-CaM dissociation, and increased phosphorylation of CaMKii.

(a) Schematic of the RAS C-terminal HVR domain. The first 165 amino acids, which determine the binding of RAS proteins to GTP/GDP, regulatory factors, and signaling effectors, are highly homologous among RAS isoforms. KRAS-4B, herein abbreviated KRAS, has a unique HVR domain containing a polylysine sequence followed by a serine residue determining the binding to CaM. Phosphorylation of KRAS at serine 181 results in KRAS-CaM dissociation and consequently increases the phosphorylation of CaMKii and decreases cancer stem cell-like properties.

(b) The CaM pulldown assay revealed that prostratin but not bryostatin I or II led to the KRAS-CaM dissociation in NIH\3T3 cells transformed with KRAS-G12V. TCL: total cell lysate. Cells were treated with each PKC activator for 48 hours before being lysed and subjected to a pulldown assay.

(c) Western blot analysis of different KRAS mutant cancer cell lines treated with prostratin at 2 μM, bryostatin I at 1 nM, and bryostatin II at 0.5 nM for 48 hours. Cells treated with prostratin but not those treated with bryostatin I or II showed increased phosphorylation of CaMKii.

(d) – (e) Ras RBD pulldown followed by western blotting for phosphoserine with different

monoclonal antibodies. Prostratin treatment at 2 μM for 24 hours resulted in specific phosphorylation of KRAS at serine 181. The pulldown of active HRAS did not contain phosphorylated serine residues. (e) KRAS with the S181A mutation showed resistance to prostratin-induced phosphorylation.

(f) Prostratin at 2 μM but not bryostatin II at 0.5 nM increased serine phosphorylation in KRAS-transformed NIH\3T3 cells. Cells were treated with the compounds for 24 hours before the pulldown assay.

(g) Prostratin treatment increased the cytosolic distribution of active CaM in PANC-1 cells, as indicated by YPet activity from a cytosol-targeted FRET biosensor. The reading of YPet in each well before compound treatments was used as the baseline, and the YPet was measured again 30 minutes and 48 hours post-treatments. The percentage of increase in each well was calculated as (Reading YPet – baseline reading)/baseline reading * 100. The concentration of each compound is indicated in the figure. The representative pictures of increasing YPet positive cells in prostratin treated group are shown in the left. (n=4; * $P < 0.05$; ** $P < 0.01$) Means are with s.d. values and plotted as bars with error bars.

Fig 3. Prostratin binds and activates PKCα.

(a) *In vitro* genome-wide CRISPR/Cas9 knockout screen. PANC-1 were treated as described in the methods section. Plot showing the distribution of normalized CRISPR viability scores (prostratin treatment vs. DMSO control) for genes targeted by the sgRNAs in the library. The red dots indicate all members in the PKC family, and the blue dots indicate the genes involved in canonical RAS signaling pathways. *PRKCA*-targeting sgRNAs were negatively selected during prostratin treatment, suggesting that *PRKCA* is an essential gene to determine the survival of PANC-1 cells under prostratin treatment. The source data are provided as a Source Data file.

(b) Scheme of the CETSA procedure used to examine the binding of PKC isozymes to ligands (prostratin or bryostatin) (left panel). (Left panel) CETSA followed by western blot analysis suggested that prostratin had a better ability to bind and stabilize intracellular PKCα than did bryostatin II in two different KRAS mutant pancreatic cancer cell lines. PANC-1 cells were treated for 48 hours and Panc 02.13 were treated for 15 minutes.

(c) Cell fractionation followed by western blot analysis suggested at differential membrane translocation of PKCα in PANC-1 cells in response to prostratin (2 μM) or bryostatin I (1 nM) or byrostatin II (0.5 nM) treatment.

(d) Immunoflourescence staining for PKCα (indicated in red) in SU86.86 cells treated with prostratin at 2 μM or bryostatin II at 0.5 nM for 24 hours. Prostratin-treated cells exhibited visible membrane-localized PKCα, whereas those treated with bryostatin II exhibited cytoplasmic PKCα.

(e) Immunoflourescence staining for PKCα (red) and PKCδ (green) in SU86.86 cells treated with prostratin at 2 μM for 24 hours.

Fig 4. KRAS acts as a substrate of PKCα upon stimulation with prostratin.

(a) Immunoprecipitation of phosphoserine PKC substrates revealed that KRAS was one of these substrates upon prostratin-induced activation. A point mutation at serine 181 of KRAS blocked this interaction.

(b) RBD pulldown followed by western blotting for phosphoserine indicated that KRAS but not NRAS interacts with and binds to PKCα in Rasless MEFs. Cells were treated with the indicated compounds for 24 hours before the pulldown assay (TCL: total cell lysate).

(c) In an assay similar to that in (b), KRAS interacted with and bound to PKCα but not PKCδ in SU86.86 cells treated with prostratin at 2 μM for 24 hours.

(d) Immunoprecipitation of HA tags in 293T cells co-transfected with HA-tagged PKCα expressing constructs and oncogenic RAS constructs at a 1:2 ratio suggested the interaction of PKCα and

KRAS. Such interaction was absent between PKCα and HRAS. Due to the limitation of available antibody for probing HRAS post-immunoprecipitation, pan-RAS antibody that can detect all RAS isoforms was used to indicate the expression of HRAS.

Fig 5. The expression of PKCα determines the responsiveness of KRAS mutant cancer cells to prostratin.

(a) Western blot analysis confirmed knockout of PKCα by CRISPR/Cas9 and re-expression of PKCα by re-introduction of wild-type PKCα (Horizon clone #OHS5899-202625016) in PANC-1 cells.

(b) CaM pulldown followed by western blotting suggested that the KRAS-CaM interaction was not disrupted upon prostratin treatment in PANC-1 cells with PKCα knockout. Cells with re-expression of PKCα responded to prostratin and showed KRAS-CaM dissociation. Cells were treated with prostratin at 2 μM for 24 hours before the pulldown assay.

(c) Ras RBD pulldown followed by western blotting for phosphoserine suggested loss of endogenous phosphorylated KRAS in PANC-1 cells with PKCα knockout. Re-expression of PKCα restored the phosphorylation of KRAS in PANC-1 cells.

(d) A colony formation assay with crystal violet staining was used to evaluate the effects of prostratin treatment on the long-term survival and proliferation of PANC-1 cells with PKCα knockout and with or without re-expression of PKCα. Cells were seeded at 100 cells per well and cultured in complete medium with the indicated compounds for 14 days until visible colonies formed.

(e) Western blot analysis confirmed the overexpression of PKCα in MIA PaCa-2 cells, which do not have endogenous expression of PKCα.

(f) CellTiter-Glo assay to evaluate the viability of MIA PaCa-2 cells with or without PKCα overexpression after treatment with prostratin for 72 hours. (n=6; **** $P < 0.0001$) Means are with s.d. values and plotted as bars with error bars.

(g) Colony formation assay followed by crystal violet staining in MIA PaCa-2 cells treated with prostratin.

Fig 6. Over-expression of PKCα or expressing constitutively active PKCα inhibits the growth and induces senescence in KRAS mutant cancer cells.

(a) Colony formation assay with visualization by crystal violet staining showed the inhibitory effect of constitutively active PKCα on the long-term growth of PANC-1 cells. The same number of cells was seeded in 6-well plates, and the cells were then transfected with constitutively active PKCα. Twelve hours post transfection, the cells were returned to complete medium for culture. The cells were stained for crystal violet on the 10th day post transfection. The experiment was repeated for four times, the crystal violet was dissolved, and the intensity of staining was quantified at absorbance 570 nm. (n=4; **** $P < 0.0001$). Means are with s.d. values and plotted as bars with error bars.

(b) Tumor growth curve of xenograft tumors derived from PANC1 cells. Error bar here indicate standard error of the mean (SEM). (n=6; ** $P < 0.01$) The images of mice bearing subcutaneous tumors are shown in the right. Tumors derived from control cells were circled in blue, and tumors from knockout group were circled in red. The images of actual and visible tumors are shown in the bottom right.

(c) Cytosolic distribution of active CaM, indicated as YPet activity from a cytosol-targeted FRET biosensor, in the cells co-transfected with biosensor and PKCα expressing constructs. The YPet in each well was measured 48 hours post-transfection, and the reading was normalized by the number of viable cells per well. (n=4; ** $P < 0.01$; *** $P < 0.001$; **** $P < 0.0001$) Means are with s.d. values and plotted as bars with error bars.

(d) β-Galactosidase staining was used to identify PANC-1 cells undergoing senescence expressing different levels of constitutively active PKCα. The cells were stained on the 6th day post transfection of active PKCα. The number of senescent cells was counted manually in a double-

blind manner. (n=4; ** P < 0.01; **** P < 0.0001)

(e) Western blot analysis confirmed the ectopic expression of HA-tagged PKCα and indicated that tumor cells treated with prostratin treatment or expressing active PKCα (PKCα-CAT) had increased p21 protein level.

(f) Percentage of β-galactosidase positive cells, stained with CellEvent™ Senescence Green and measured by flow cytometry analysis, in the KRAS mutant tumor cells. The cells were first transfected with siRNA against PTPN14 and treated with 2 μM prostratin for 5 days to induce senescence. Non-targeting siRNA was used as control. (n=3; * P < 0.05; ** P < 0.01; *** P < 0.001)

(g) (Left panel) Quantitative PCR indicated the expression level of the expression of p21 (*CDKN1A*) mRNA in tumor cells where indicated genes were knocked down by siRNA. PANC-1 cells were transfected with siRNA, followed by the treatment of prostratin at 2 μM for 3 days before RNA extraction. (n=3; ** P < 0.01; *** P < 0.001; **** P < 0.0001) Means are with s.d. values and plotted as bars with error bars. (Right panel) Nucleus extraction followed by western blot analysis revealed the increased nucleus-localized p21 protein in the MIA PaCa2 cells expressing wild type PKCα upon the treatment with prostatin at 2μM for 72 hours. Knocking down siPTPN14 suppressed the increase in p21 caused by prostratin treatment. Histone H1B was used as a loading control.

(h) Colony formation assay followed by crystal violet staining suggested that knocking down PTPN14 by siRNA rescued the growth inhibition caused by activation of PKCα in KRAS mutant cancer cells. The cells were transfected with siRNAs, followed by treatment of prostratin at 2 μM or transfected with constitutively active PKCα. The cells were allowed to grow for 10 days or until visible colonies formed. The cells were then fixed and stained with crystal violet, later dissolved in 1% SDS for further determination of colony density. (n=4; * P < 0.05; ** P < 0.01; *** P < 0.001; **** P < 0.0001) Means are with s.d. values and plotted as bars with error bars.

Fig 7. Activation of PKCα induces the expression and secretion of CCL3, CCL4, and/or CXCL1 in KRAS mutant tumor cells.

(a) Detection of human cytokines and chemokines by using Proteome Profiler Human Cytokine Array Kit in human pancreatic cancer cells expressing constitutively active form of PKCα. The cells were first transfected with PKCα-CAT, and the total cell lysates were harvested 72 hours post-transfection for the antibody array analysis. The intensity of each dot was determined by ImageJ and normalized by the control dots. Cells expressing empty vector were used as control.

(b) ELISA used to detect the secretion of CXCL1 from cells with activated PKCα to the culture supernatant. Cells were treated with prostratin at 2 μM or transfected with constitutively active form of PKCα. Culture supernatant was harvested 72 hours post-treatment or transfection. Cells transfected with empty vector and treated with DMSO were used as control. Prior to ELISA, culture supernatant was normalized with the number of attached cells at the time of harvesting. (n=3; * $P < 0.05$; ** $P < 0.01$; **** $P < 0.0001$) Means are with s.d. values and plotted as bars with error bars.

(c) Colony formation assay followed by crystal violet staining in the tumor cells expressing active PKCα with treatment of neutralizing antibodies as indicated. Cells seeded in 12 well plates were transfected to ectopically express constitutively active mutant of PKCα, followed by treatment of indicated neutralizing antibody at 0.5 μg/mL till the visible colonies formed. (n=3; * $P < 0.05$; ** $P < 0.01$) Means are with s.d. values and plotted as bars with error bars.

Extended Data Fig 1.

(a) Quantitation of spheres grown in 3D culture in response to treatment with prostratin, bryostatin I or bryostatin II. The viability of spheres was normalized to that in the control (DMSO-treated) group. (n=6; * $P < 0.05$, *** $P < 0.001$) Means are with s.d. values and plotted as bars with error bars.

(b) Representative images of spheres derived from the KRAS mutant cancer cell line Panc02.13 treated with different compounds. Images were acquired with a high-power objective (200X magnification).

(c) CellTiter-Glo assay to quantify the viability of PANC-1 cells after treatment with prostratin at different doses. DMSO-treated cells were used as the normalization control. (n=6)

(d) Western blot analysis of apoptosis markers in different KRAS mutant cancer cells treated with prostratin for 16-18 hours.

(e) β-Galactosidase staining was used to indicate the senescent cells among human pancreatic epithelial cells expressing oncogenic HRAS or KRAS and treated with prostratin at 2 μM for 6 days. The positively stained cells were manually counted in a double-blind manner. Twelve images of each well in a 6-well plate were acquired to calculate the mean value in each group. The error bars indicate the s.d. of three technical replicates. (n=3, *P < 0.05)

(f) Prostratin treatment at 2 μM for 6 days significantly increased the percentage of β-Galactosidase positive cells quantified by flow cytometry in two different KRAS mutant cancer cell lines. (n=4; *** P < 0.001; **** P < 0.00001)

(g) (Left panel) Representative images of SU86.86 cells exhibiting a senescent morphology after treatment with prostratin at 2 μM or with a combination of trametinib (10 nM) and palbociclib (0.1 μM) for 6 days. (Right panel) Western blots indicating the expression level of p21 in SU86.86 cells treated with the indicated compounds.

(h) Western blots for p21, lamin B1, and β-actin in PANC-1 cells treated with prostratin at 2 μM or bryostatin II at 0.5 nM for 7 days.

Extended Data Fig 2.

(a) Western blots indicating the expression levels of the stem cell markers CD44 and Sox9 along with phosphorylated CaMKii in Panc02.13 cells treated with PMA at 100 nM, prostratin at 2 μM, or bryostatin II at 0.5 nM for 48 hours.

(b) Western blotting for CD44 in PANC-1 and Panc02.13 cells treated with prostratin at two different concentrations for 48 hours.

(c) Cell fractionation assay to define the subcellular localization of KRAS in PANC-1 cells treated with prostratin at 2 μM, bryostatin I at 1 nM, or bryostatin II at 0.5 nM.

(d) Western blotting for phospho-ERK in cells treated with prostratin at 2 μM or bryostatin II at 0.5 nM for 48 hours. Total ERK was used as the internal control.

Extended Data Fig 3.

Cell fractionation assay followed by western blot analysis to define the subcellular localization of PKCα, PKCδ, or KRAS in Panc02.13 cells treated with prostratin at 2 μM or bryostatin II at 0.5 nM.

Extended Data Fig 4.

Summary of the KRAS mutations, the response to prostratin, and expression level of each PKC isozyme in the cancer cell lines used in this study. mRNA expression levels were obtained from the Cancer Cell Line Encyclopedia (Broad Institute, 2019).

Extended Data Fig 5.

(a) CellTiter-Glo assay to determine the viability of PANC-1 cells with modified expression of PKCα after prostratin treatment. Cells were treated for 72 hours. DMSO was used as the control. (n=6, *** $P < 0.001$, **** $P < 0.0001$) Means are with s.d. values and plotted as bars with error bars.

(b) Western blot analysis to evaluate the endogenous expression of PKCα and PKCδ in different KRAS mutant cancer cell lines.

(c) Colony formation assay followed by crystal violet staining in MIA PaCa-2 and Panc03.27 cells treated with the indicated compounds. Two hundred cells per well were seeded in complete medium containing the compounds.

Extended Data Fig 6.

(a) Western blot analysis confirmed the expression level of constitutively active PKCα in PANC-1 cells with knockout of endogenous PKCα. A HA tag was used to indicate specific expression of constitutively active PKCα. Expression of constitutively activated PKCα corresponds with an increase in the phosphorylation level of CaMKii (T286).

(b) Colony formation visualized by crystal violet staining in a series of tumor cells with wild type or mutant KRAS which ectopically expressed constitutively active mutant form of PKCα. (n=4, *** $P < 0.001$) Means are with s.d. values and plotted as bars with error bars.

(c) Cell viability in the cells expressing wild type of constitutively active PKCα. (n=4; * $P < 0.05$; **** $P < 0.0001$) Means are with s.d. values and plotted as bars with error bars.

(d) Tumor growth curve of xenograft tumors derived from MIA PaCa2 cells. Error bar here indicate standard error of the mean (SEM). (n=5; ** $P < 0.01$)

(e) Western blot analysis confirmed the expression of HA-tagged PKCα and the increased expression of p21 in PANC-1 cells where the endogenous PKCα had been knocked out by CRISPR/Cas9.

(f) Quantitative PCR indicated that the expression level of PKCα affected the expression of p21 (CDKN1A) at mRNA level in tumor cells. (n=3; ** $P < 0.01$; *** $P < 0.001$; **** $P < 0.0001$) Means are with s.d. values and plotted as bars with error bars.

(g) Nucleus extraction followed by western blot analysis revealed the increased nucleus-localized p21 level in the cells expressing constitutively active PKCα (CAT). Histone H1B was used as the loading control.

(h) Quantitative PCR indicated the expression of p21 (CDKN1A) at mRNA level in cells treated with 2 μM prostratin, followed by the treatment of W7 at 25 μM for 72 hours. (n=3; ** $P < 0.01$; *** $P < 0.001$; **** $P < 0.0001$) Means are with s.d. values and plotted as bars with error bars.

(i) Different pancreatic tumor cells with activated and/or overexpressed PKCα were subjected to

nucleus extraction followed by Western blot analysis for CAMTA1. Histone H1B was used as a loading control.

(j) (Left panel) The representative images of CAMTA1 IHC in mice. Mice bearing KRAS-driven papillomas were treated with vehicle (left) or prostratin (right) for 21 days. (Right panel?) Tumor were stained and counted for CAMTA1 in a double-blind manner. Nuclear CAMTA1: control 2.79±4.2%; prostratin 89.7±15.1% (n=4; ***P < 0.001)

Extended Data Fig 7.

(a) Detection of human cytokines and chemokines by using Proteome Profiler Human Cytokine Array in Panc02.13 cells treated with prostratin at 2 μM or with a combination of trametinib (10 nM) and palbociclib (0.1 μM) for 72 hours.

(b) ELISA to detect the secretion of CXCL1 by Panc02.13 with activated PKCα to the culture supernatant. (n=3; **** P < 0.0001)

(c) Quantitative PCR indicated that the expression of CXCL1 at mRNA level in human pancreatic cancer cells treated with prostratin at 2 μM or transfected with PKCα-CAT followed by the treatment of W7 at 25 μM. RNA was extracted 48 hours post-transfection and/or treatment. (n=3; **** P < 0.0001) Means are with s.d. values and plotted as bars with error bars.

(d) Quantitative PCR indicated that the expression of CXCL1 at mRNA level in PANC-1 cells with siRNA knockdown of PTPN14 and treatment of prostratin at 2 μM. (n=3; **** P < 0.0001) Means are with s.d. values and plotted as bars with error bars.

(e) – (f) ELISA to detect CCL3 or CCL4 secreted from Panc02.13 with activated PKCα to the supernatant. (n=3; ** P < 0.01; **** P < 0.0001) Means are with s.d. values and plotted as bars with error bars.

(g) Colony formation visualized by crystal violet staining in NCI-H647 cells expressing active form of PKCα and treated with anti-CXCL1 antibody. (n=4; ** P < 0.01) Means are with s.d. values and plotted as bars with error bars.

Graphic abstract

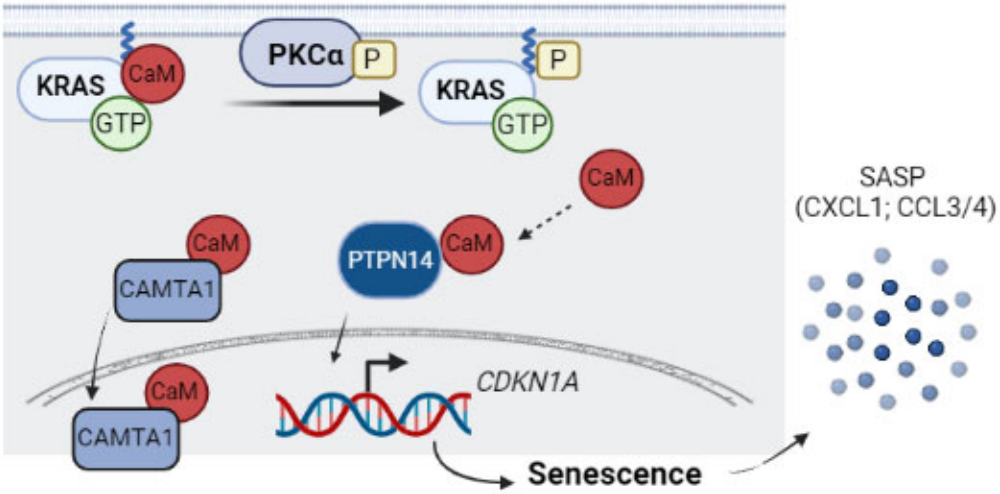

Fig. 1

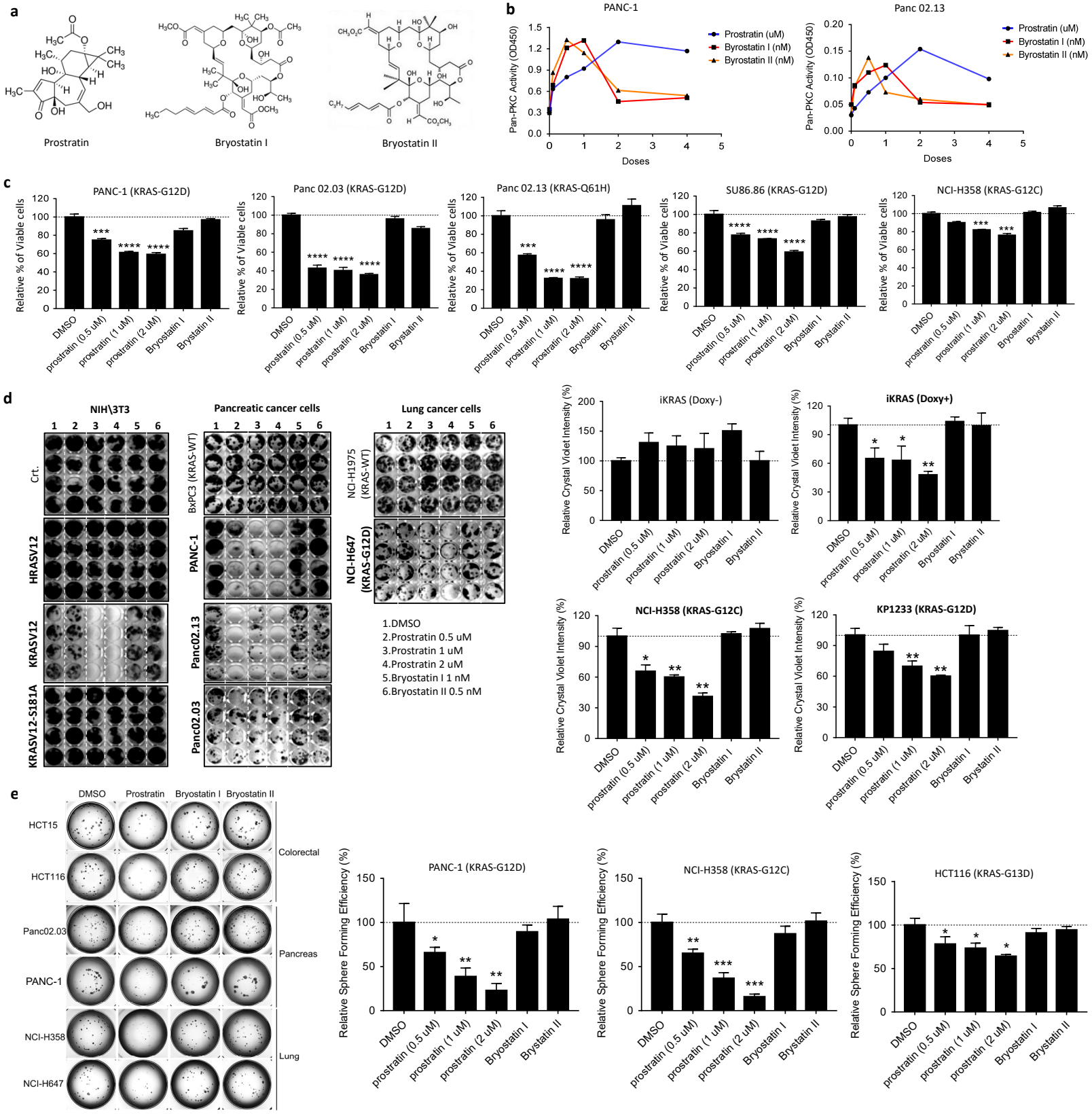
a
Prostratin
Bryostatin I
Bryostatin II
b
PANC-1
Panc 02.13
Pan-PKC Activity (OD450)
Doses
Prostratin (uM)
Byrostatin I (nM)
Byrostatin II (nM)
c
PANC-1 (KRAS-G12D)
Panc 02.03 (KRAS-G12D)
Panc 02.13 (KRAS-Q61H)
SU86.86 (KRAS-G12D)
NCI-H358 (KRAS-G12C)
Relative % of Viable cells
DMSO
prostratin (0.5 uM)
prostratin (1 uM)
prostratin (2 uM)
Bryostatin I
Brystatin II
d
NIH\3T3
Pancreatic cancer cells
Lung cancer cells
Crt.
HRASV12
KRASV12
KRASV12-S181A
BxPC3 (KRAS-WT)
PANC-1
Panc02.13
Panc02.03
NCI-H1975 (KRAS-WT)
NCI-H647 (KRAS-G12D)
1.DMSO
2.Prostratin 0.5 uM
3.Prostratin 1 uM
4.Prostratin 2 uM
5.Bryostatin I 1 nM
6.Bryostatin II 0.5 nM
iKRAS (Doxy-)
iKRAS (Doxy+)
NCI-H358 (KRAS-G12C)
KP1233 (KRAS-G12D)
Relative Crystal Violet Intensity (%)
e
DMSO
Prostratin
Bryostatin I
Bryostatin II
HCT15
HCT116
Colorectal
Panc02.03
PANC-1
Pancreas
NCI-H358
NCI-H647
Lung
PANC-1 (KRAS-G12D)
NCI-H358 (KRAS-G12C)
HCT116 (KRAS-G13D)
Relative Sphere Forming Efficiency (%)

Fig. 2

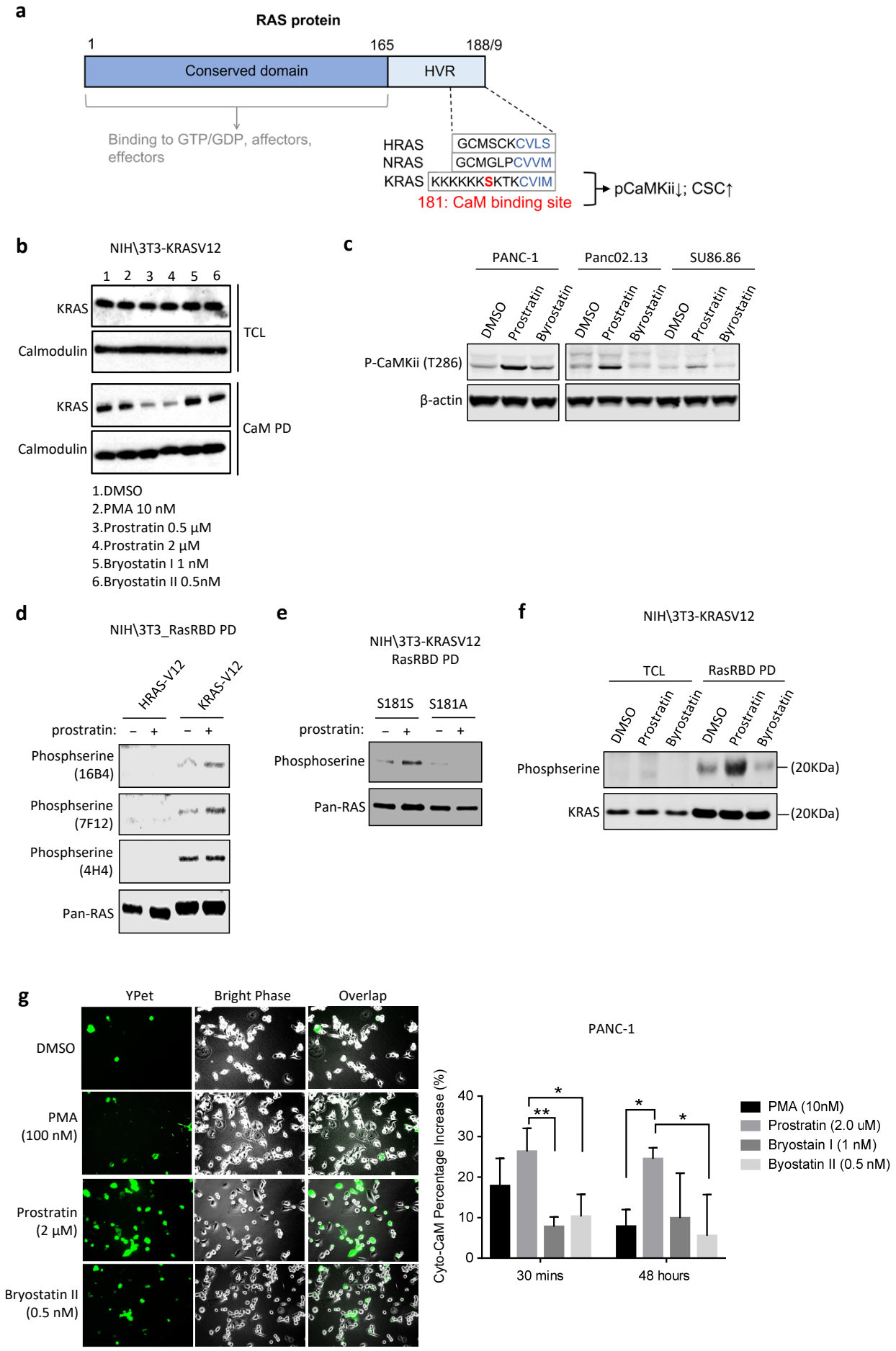
a
RAS protein
1
165
188/9
Conserved domain
HVR
Binding to GTP/GDP, affectors, effectors
HRAS GCMSCKCVLS
NRAS GCMGLPCVVM
KRAS KKKKKKKSKTKCVIM
181: CaM binding site
pCaMKii↓; CSC↑
b
NIH\3T3-KRASV12
1 2 3 4 5 6
KRAS
Calmodulin
TCL
KRAS
Calmodulin
CaM PD
1.DMSO
2.PMA 10 nM
3.Prostratin 0.5 μM
4.Prostratin 2 μM
5.Bryostatin I 1 nM
6.Bryostatin II 0.5nM
c
PANC-1
Panc02.13
SU86.86
DMSO
Prostratin
Byrostatin
P-CaMKii (T286)
β-actin
d
NIH\3T3_RasRBD PD
HRAS-V12
KRAS-V12
prostratin: – + – +
Phosphserine (16B4)
Phosphserine (7F12)
Phosphserine (4H4)
Pan-RAS
e
NIH\3T3-KRASV12
RasRBD PD
S181S
S181A
prostratin: – + – +
Phosphoserine
Pan-RAS
f
NIH\3T3-KRASV12
TCL
RasRBD PD
DMSO
Prostratin
Byrostatin
Phosphserine
KRAS
(20KDa)
(20KDa)
g
YPet
Bright Phase
Overlap
DMSO
PMA (100 nM)
Prostratin (2 μM)
Bryostatin II (0.5 nM)
PANC-1
Cyto-CaM Percentage Increase (%)
40
30
20
10
0
*
**
*
*
30 mins
48 hours
PMA (10nM)
Prostratin (2.0 uM)
Bryostain I (1 nM)
Byostatin II (0.5 nM)

Fig. 3

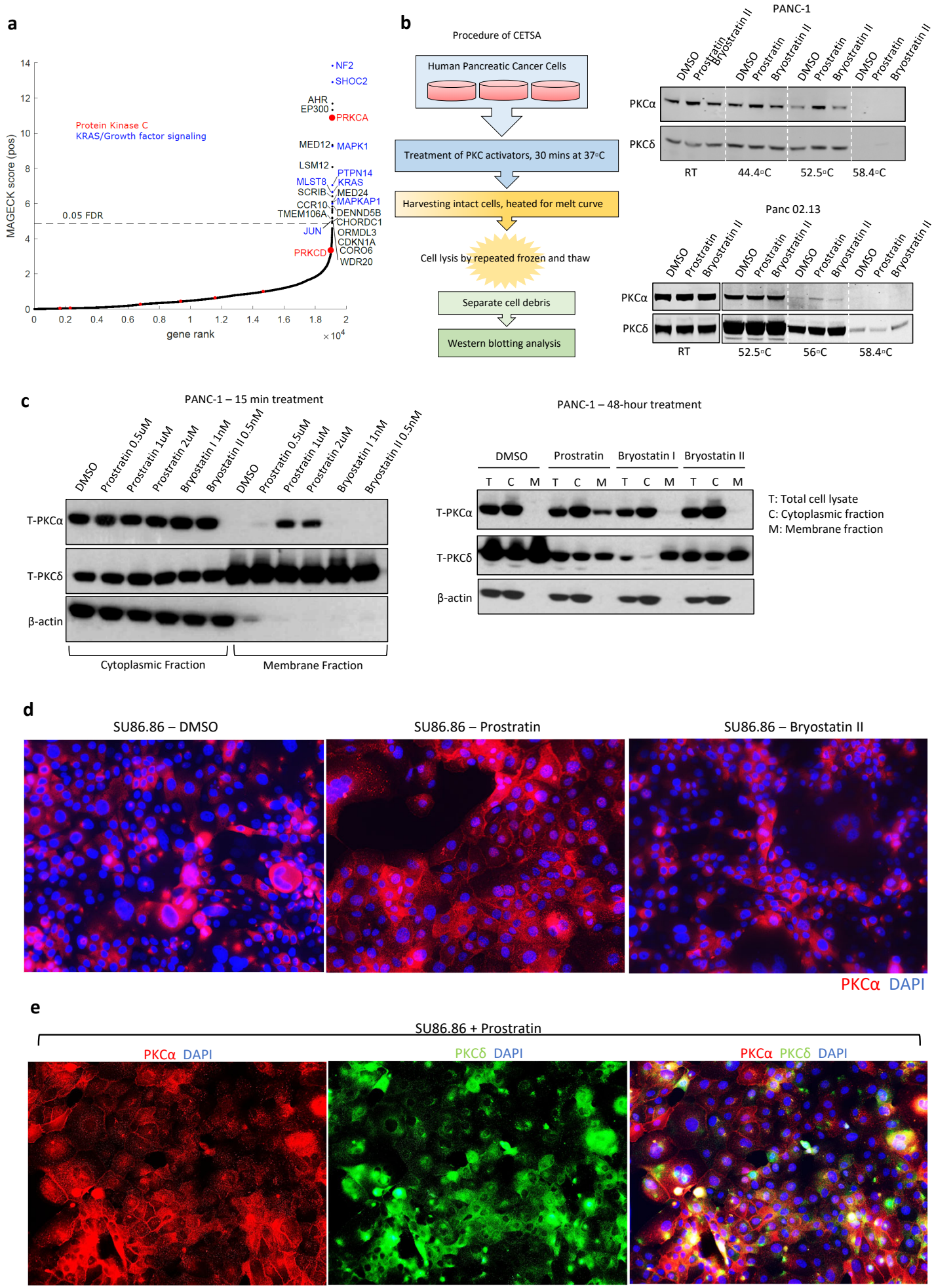
a
MAGECK score (pos)
gene rank
0.05 FDR
Protein Kinase C
KRAS/Growth factor signaling
NF2
SHOC2
AHR
EP300
PRKCA
MED12
MAPK1
LSM12
PTPN14
MLST8
KRAS
SCRIB
MED24
CCR10
MAPKAP1
TMEM106A
DENND5B
CHORDC1
JUN
ORMDL3
CDKN1A
PRKCD
CORO6
WDR20
b
Procedure of CETSA
Human Pancreatic Cancer Cells
Treatment of PKC activators, 30 mins at 37°C
Harvesting intact cells, heated for melt curve
Cell lysis by repeated frozen and thaw
Separate cell debris
Western blotting analysis
PANC-1
DMSO
Prostratin
Bryostatin II
PKCα
PKCδ
RT
44.4°C
52.5°C
58.4°C
Panc 02.13
56°C
c
PANC-1 – 15 min treatment
DMSO
Prostratin 0.5uM
Prostratin 1uM
Prostratin 2uM
Bryostatin I 1nM
Bryostatin II 0.5nM
T-PKCα
T-PKCδ
β-actin
Cytoplasmic Fraction
Membrane Fraction
PANC-1 – 48-hour treatment
Prostratin
Bryostatin I
T
C
M
T: Total cell lysate
C: Cytoplasmic fraction
M: Membrane fraction
d
SU86.86 – DMSO
SU86.86 – Prostratin
SU86.86 – Bryostatin II
PKCα DAPI
e
SU86.86 + Prostratin
PKCα DAPI
PKCδ DAPI
PKCα PKCδ DAPI

Fig. 4

a

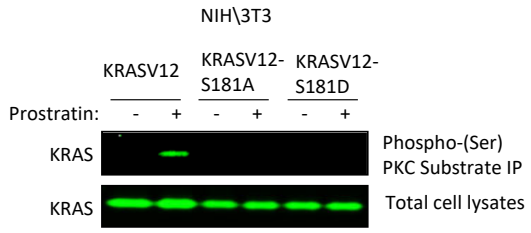
NIH\3T3
KRASV12
KRASV12-S181A
KRASV12-S181D
Prostratin: - + - + - +
KRAS
Phospho-(Ser) PKC Substrate IP
KRAS
Total cell lysates

b

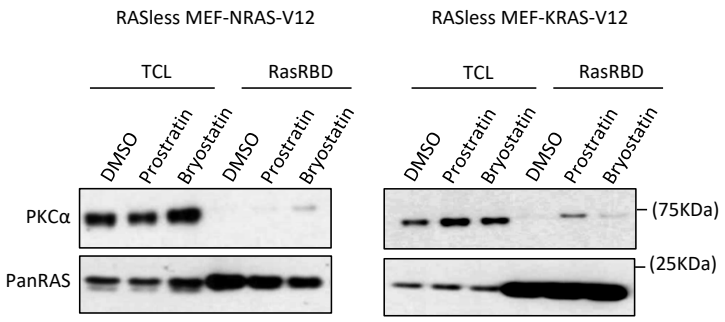
RASless MEF-NRAS-V12
RASless MEF-KRAS-V12
TCL
RasRBD
DMSO
Prostratin
Bryostatin
PKCα
PanRAS
(75KDa)
(25KDa)

c

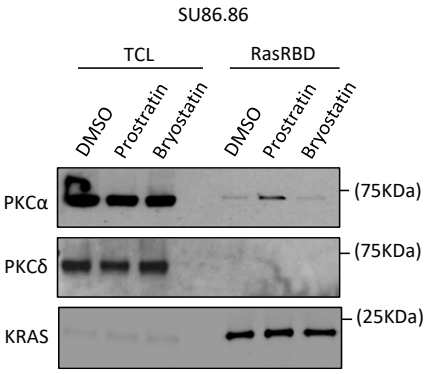
SU86.86
TCL
RasRBD
DMSO
Prostratin
Bryostatin
PKCα
PKCδ
KRAS
(75KDa)
(75KDa)
(25KDa)

d

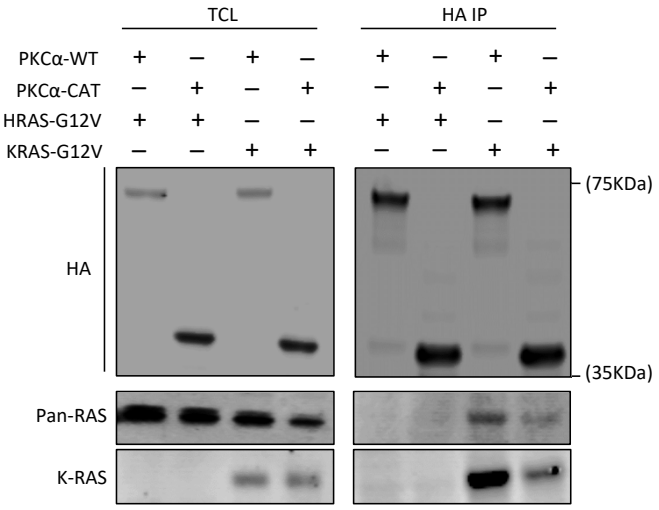
TCL
HA IP
PKCα-WT + − + − + − + −
PKCα-CAT − + − + − + − +
HRAS-G12V + + − − + + − −
KRAS-G12V − − + + − − + +
HA
Pan-RAS
K-RAS
(75KDa)
(35KDa)

Fig. 5

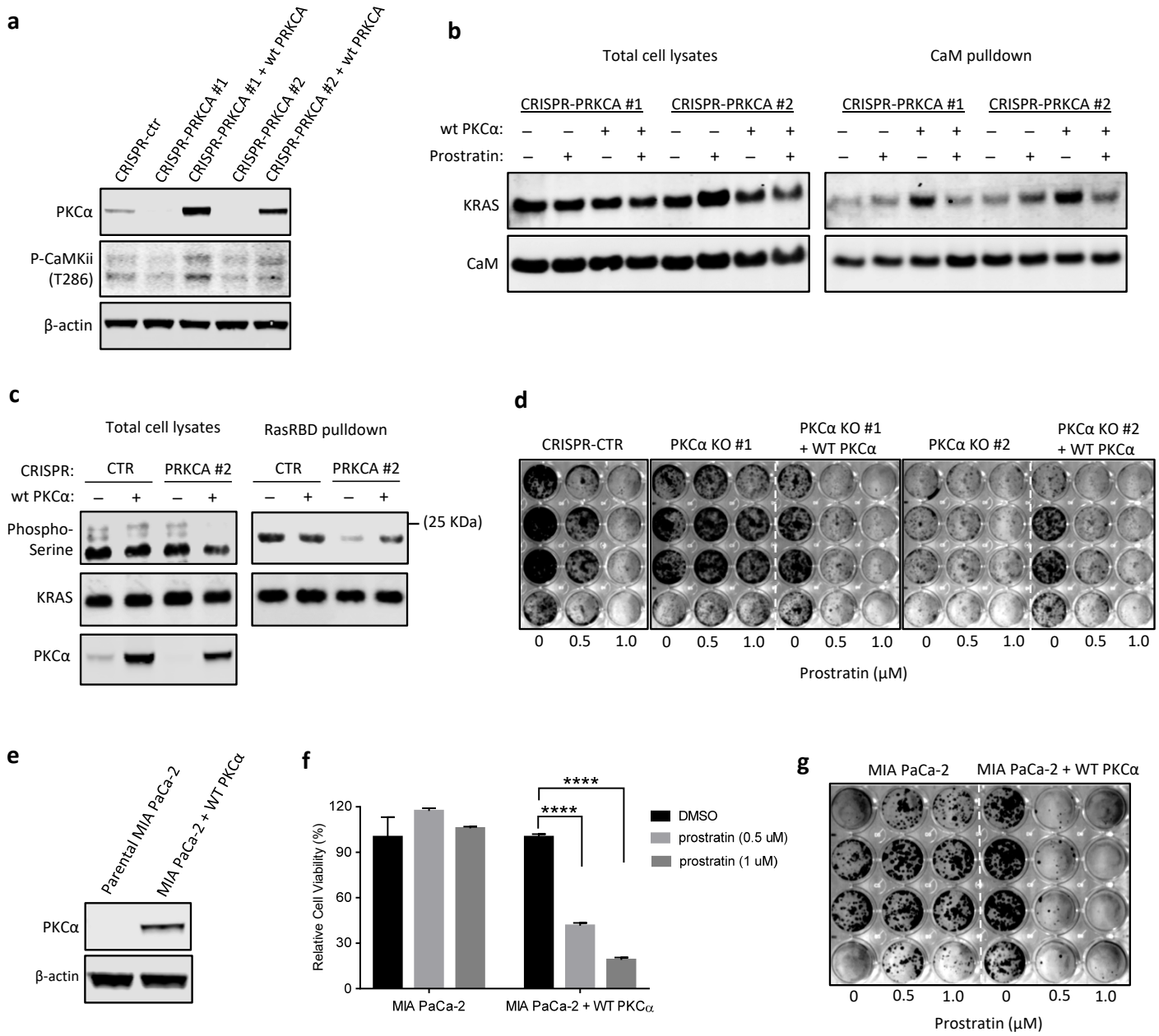
a
CRISPR-ctr
CRISPR-PRKCA #1
CRISPR-PRKCA #1 + wt PRKCA
CRISPR-PRKCA #2
CRISPR-PRKCA #2 + wt PRKCA
PKCα
P-CaMKii (T286)
β-actin
b
Total cell lysates
CaM pulldown
CRISPR-PRKCA #1
CRISPR-PRKCA #2
wt PKCα:
Prostratin:
KRAS
CaM
c
Total cell lysates
RasRBD pulldown
CRISPR:
CTR
PRKCA #2
wt PKCα:
Phospho-Serine
KRAS
PKCα
(25 KDa)
d
CRISPR-CTR
PKCα KO #1
PKCα KO #1 + WT PKCα
PKCα KO #2
PKCα KO #2 + WT PKCα
0 0.5 1.0
Prostratin (μM)
e
Parental MIA PaCa-2
MIA PaCa-2 + WT PKCα
PKCα
β-actin
f
Relative Cell Viability (%)
120
90
60
30
0
****
DMSO
prostratin (0.5 uM)
prostratin (1 uM)
MIA PaCa-2
MIA PaCa-2 + WT PKCα
g
MIA PaCa-2
MIA PaCa-2 + WT PKCα
0 0.5 1.0
Prostratin (μM)

Fig. 6

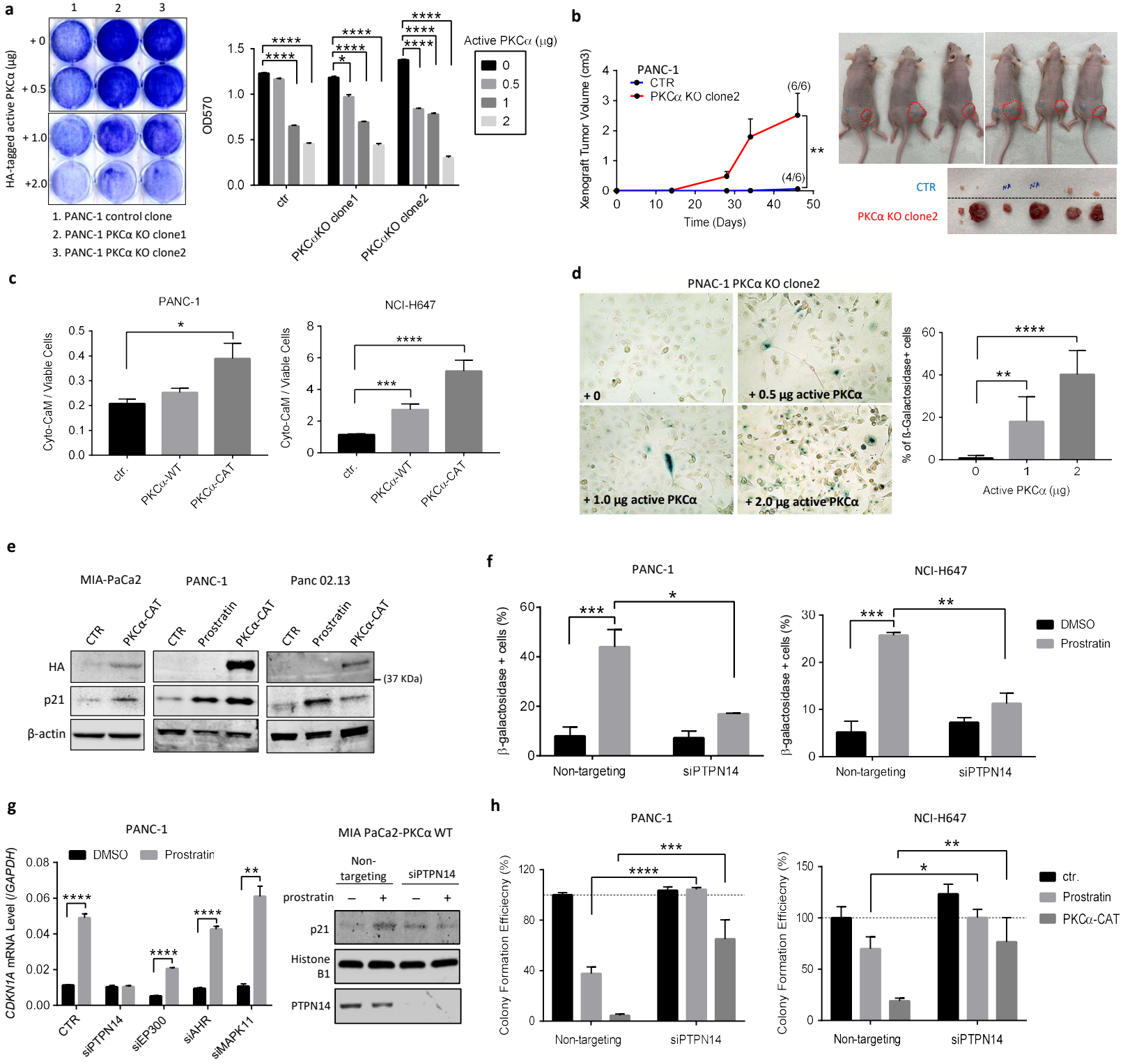
a
HA-tagged active PKCα (μg)
+ 0
+ 0.5
+ 1.0
+2.0
1. PANC-1 control clone
2. PANC-1 PKCα KO clone1
3. PANC-1 PKCα KO clone2
OD570
Active PKCα (μg)
ctr
PKCαKO clone1
PKCαKO clone2
b
Xenograft Tumor Volume (cm3)
PANC-1
CTR
PKCα KO clone2
Time (Days)
(6/6)
(4/6)
CTR
PKCα KO clone2
c
PANC-1
NCI-H647
Cyto-CaM / Viable Cells
ctr.
PKCα-WT
PKCα-CAT
d
PNAC-1 PKCα KO clone2
+ 0
+ 0.5 μg active PKCα
+ 1.0 μg active PKCα
+ 2.0 μg active PKCα
% of ß-Galactosidase+ cells
Active PKCα (μg)
e
MIA-PaCa2
PANC-1
Panc 02.13
CTR
PKCα-CAT
Prostratin
HA
p21
β-actin
(37 KDa)
f
PANC-1
NCI-H647
β-galactosidase + cells (%)
Non-targeting
siPTPN14
DMSO
Prostratin
g
PANC-1
DMSO
Prostratin
CDKN1A mRNA Level (/GAPDH)
CTR
siPTPN14
siEP300
siAHR
siMAPK11
MIA PaCa2-PKCα WT
Non-targeting
siPTPN14
prostratin
p21
Histone B1
PTPN14
h
PANC-1
NCI-H647
Colony Formation Efficiecny (%)
Non-targeting
siPTPN14
ctr.
Prostratin
PKCα-CAT

Fig. 7

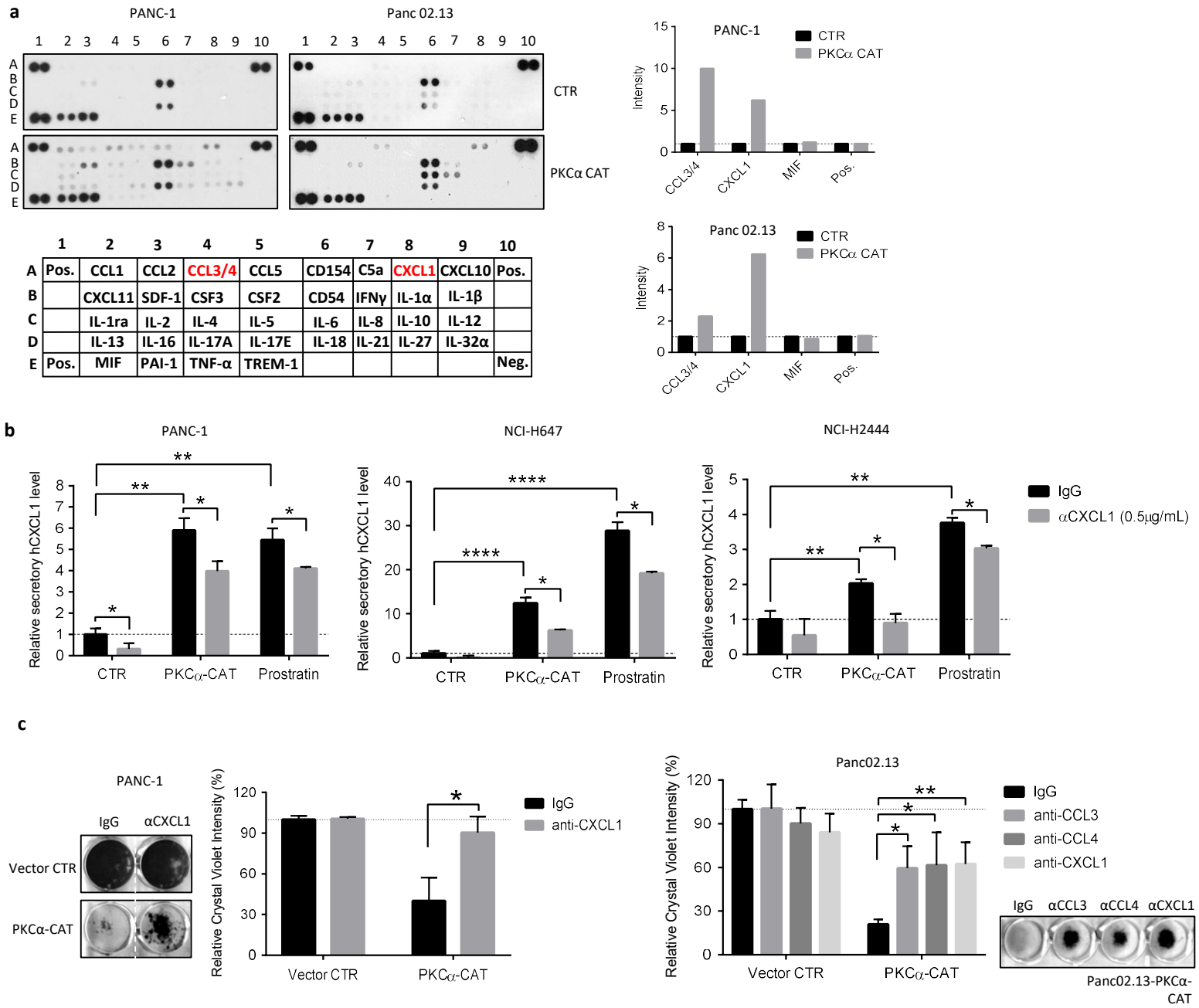

	1	2	3	4	5	6	7	8	9	10
A	Pos.	CCL1	CCL2	CCL3/4	CCL5	CD154	C5a	CXCL1	CXCL10	Pos.
B		CXCL11	SDF-1	CSF3	CSF2	CD54	IFNγ	IL-1α	IL-1β	
C		IL-1ra	IL-2	IL-4	IL-5	IL-6	IL-8	IL-10	IL-12	
D		IL-13	IL-16	IL-17A	IL-17E	IL-18	IL-21	IL-27	IL-32α	
E	Pos.	MIF	PAI-1	TNF-α	TREM-1					Neg.

Extended Data Fig. 1

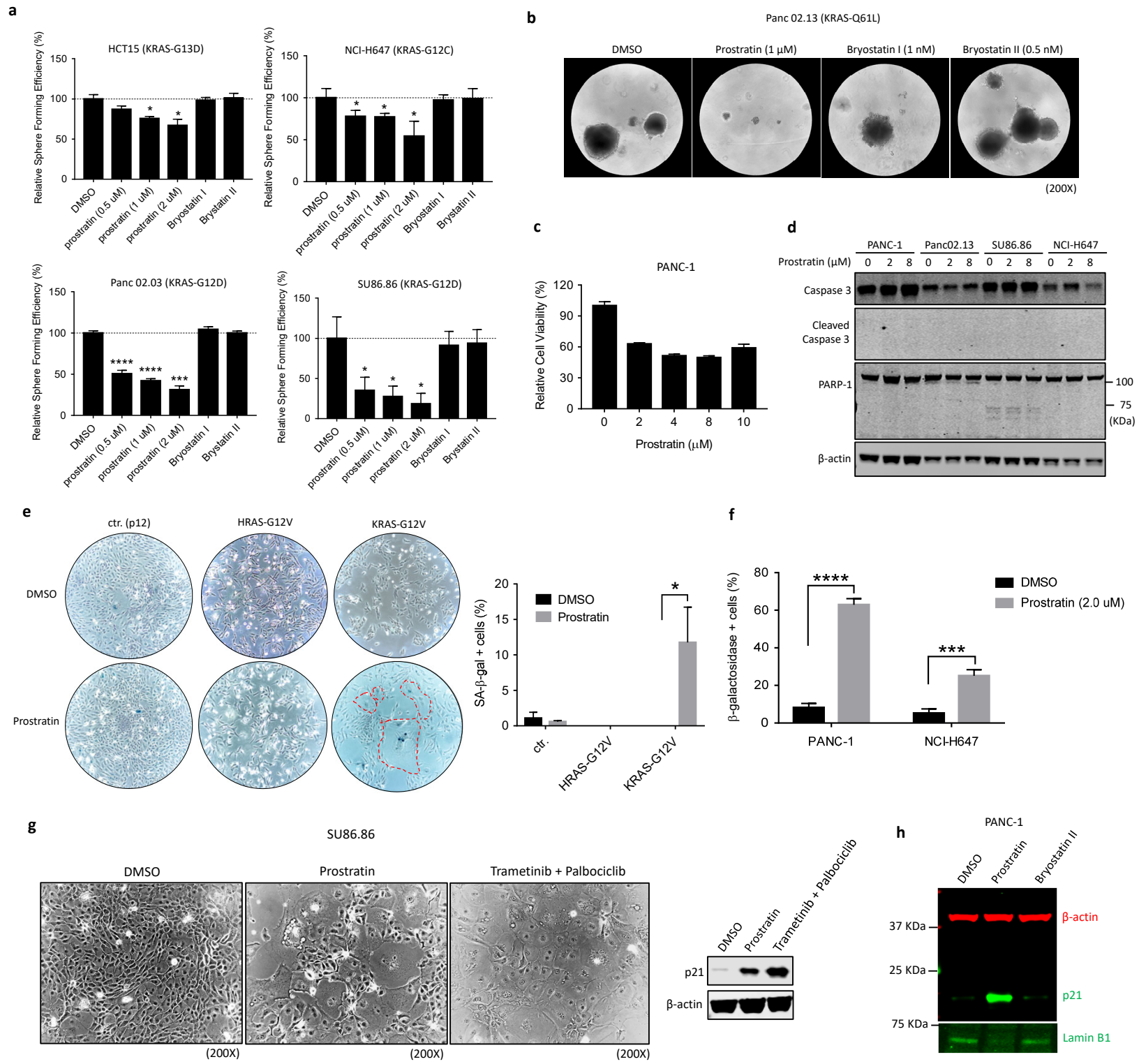

Extended Data Fig. 2

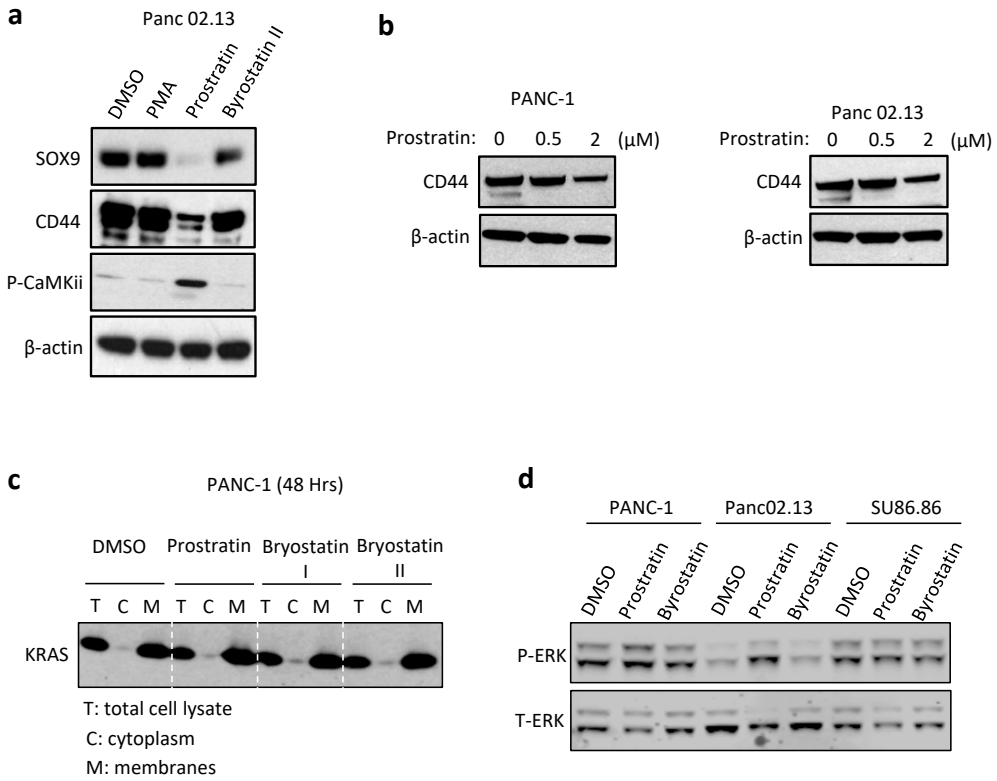

Extended Data Fig. 3

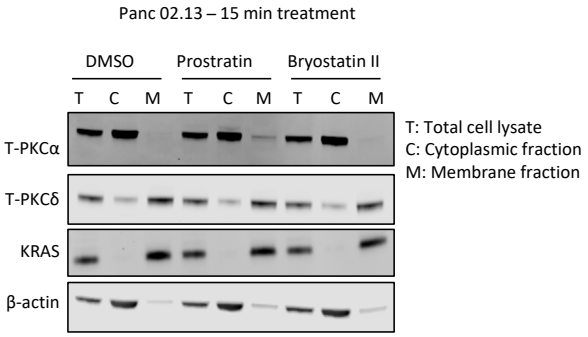

Extended Data Fig. 4

Cell line	KRAS Mutation	Prostratin Sensitivity	RNA Seq V2 RSEM normalized expression values						
			PRKCA	PRKCD	PRKCE	PRKCB	PRKCG	PRKCH	PRKCQ
BxPC3	WT	Non-responder	2.865	16.852	1.036	0.28	0.271	5.0723	0.0873
H1975	WT	Non-responder	14.518	15.286	1.678	0.01	0.243	1.279	0
PANC-1	G12D	Responder	13.533	8.133	1.000	0.0136	0.380	0.139	0.029
Panc02.03	G12D	Responder	5.165	16.641	2.530	0.024	2.029	1.661	0.546
Panc02.13	Q61H	Responder	14.397	19.674	2.138	0.013	0.359	4.249	0.021
SU86.86	G12D	Responder	13.370	12.766	4.159	0.025	0.439	5.182	1.530
NCI-H358	G12C	Responder	14.397	19.674	2.138	0.013	0.359	4.249	0.021
NCI-H647	G12C	Responder	9.823	5.789	3.136	0.014	0.008	1.718	0.305
HCT15	G13D	Responder	2.376	5.176	0.727	0.018	0.147	3.283	0.962
HCT116	G13D	Responder	4.575	15.083	1.205	0.002	0.403	2.858	0.244

Extended Data Fig. 5

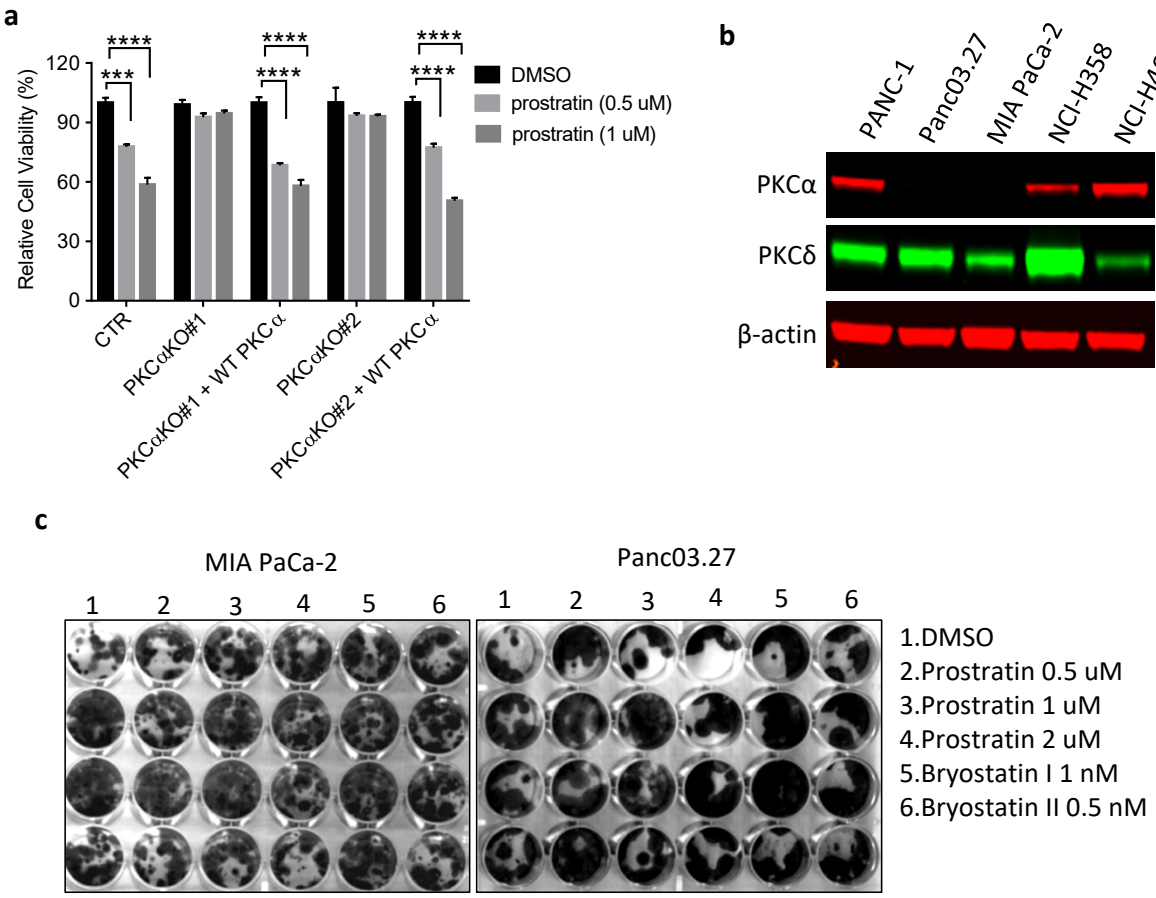

Extended Data Fig. 6

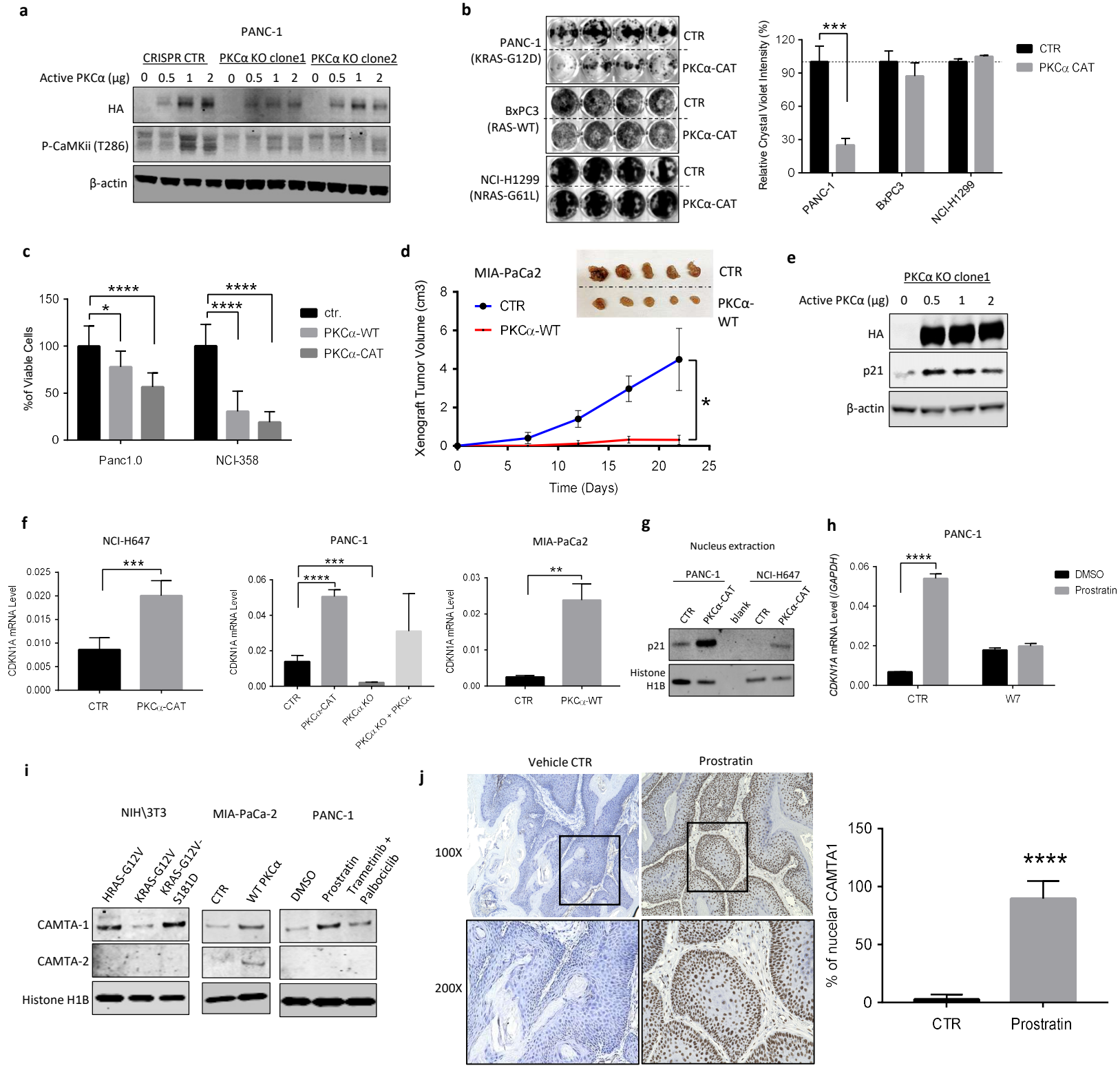
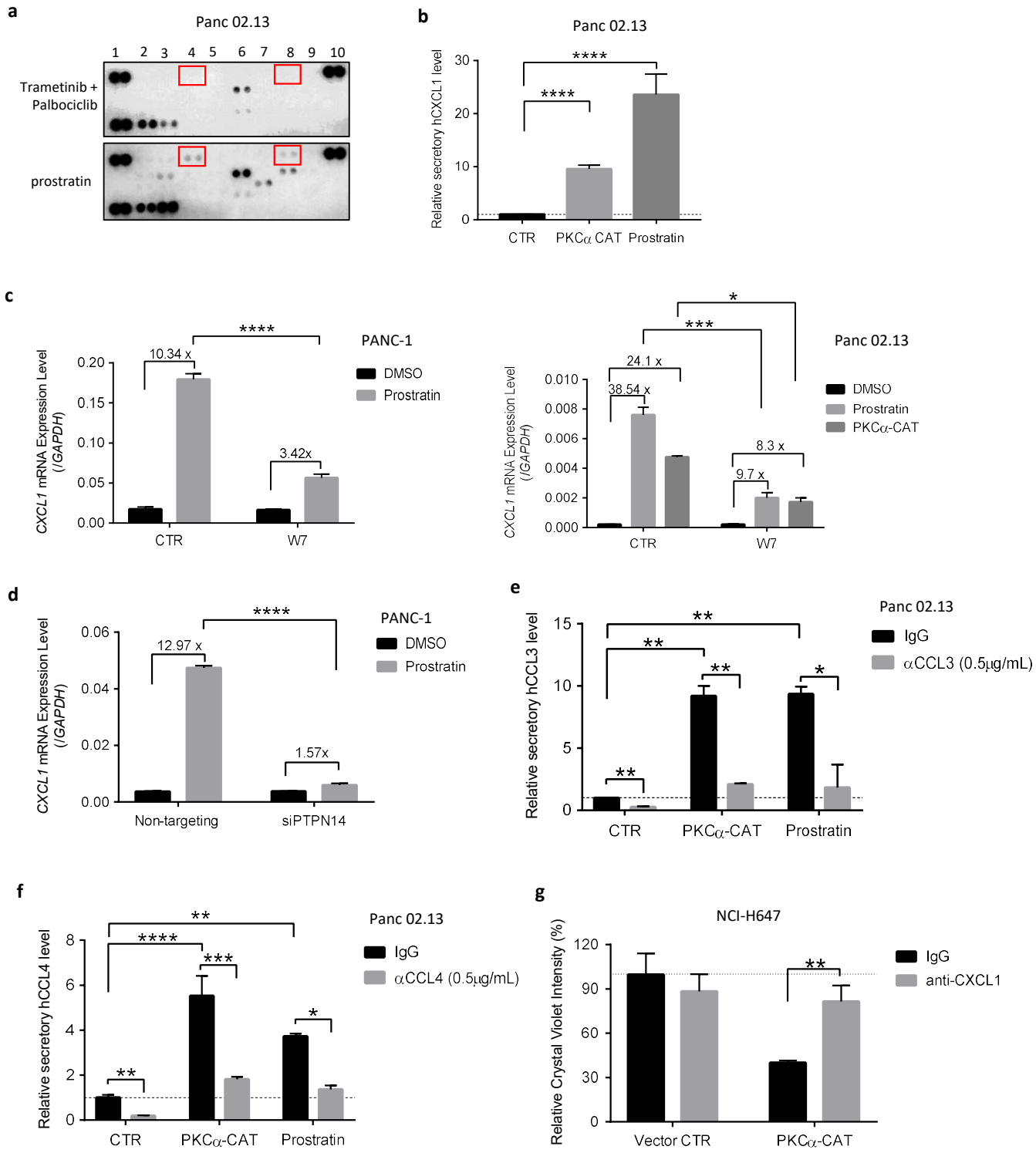
Extended Data Fig. 7